Astronomy & Astrophysics manuscript no. output
December 18, 2023

BASECOL2023 scientific content

M.L. Dubernet[1⋆], C. Boursier[1], O. Denis-Alpizar[3⋆⋆], Y.A. Ba[1], N. Moreau[1], C. M. Zwölf[1], M.A. Amor[4], D. Babikov[5], N. Balakrishnan[6], C. Balança[1], M. Ben Khalifa[7], A. Bergeat[2], C.T. Bop[8], L. Cabrera-González[9], C. Cárdenas[10,11], A. Chefai[4], P. J. Dagdigian[12], F. Dayou[1], S. Demes[8], B. Desrousseaux[8], F. Dumouchel[13], A. Faure[14], R. C. Forrey[15], J. Franz[16], R. M. García-Vázquez[2,26], F. Gianturco[17], A. Godard Palluet[8], L. González-Sánchez[19], G. C. Groenenboom[20], P. Halvick[2], K. Hammami[4], F. Khadri[4], Y. Kalugina[8], I. Kleiner[21], J. Kłos[22,23], F. Lique[8], J. Loreau[7], B. Mandal[5], B. Mant[17], S. Marinakis[18], D. Ndaw[24], P. Pirlot Jankowiak[8], T. Price[15], E. Quintas-Sánchez[27], R. Ramachandran[13,28], E. Sahnoun[4], C. Santander[3], P. C. Stancil[25], T. Stoecklin[2], J. Tennyson[29], F. Tonolo[30,31], R. Urzúa-Leiva[3], B. Yang[25], E. Yurtsever[32], and Michal Żółtowski[8,13]

(Affiliations can be found after the references)

Received Month day, year; accepted Month day, year

ABSTRACT

Context. The global context of making numerous data produced by researchers available requires collecting and organising the data, assigning meaningful metadata, and presenting the data in a meaningful and homogeneous way. The BASECOL database, which collects inelastic rate coefficients for application to the interstellar medium and to circumstellar and cometary atmospheres, meets those requirements.
Aims. We aim to present the scientific content of the BASECOL2023 edition.
Methods. While the previous versions relied on finding rate coefficients in the literature, the current version is populated with published results sent by the producers of data. The paper presents the database, the type of data that can be found, the type of metadata that are used, and the Virtual Atomic and Molecular Data Centre (VAMDC) standards that are used for the metadata. Finally, we present the different datasets species by species.
Results. As the BASECOL database, interconnected with the VAMDC e-infrastructure, uses the VAMDC standards, the collisional data can be extracted with tools using VAMDC standards and can be associated with spectroscopic data extracted from other VAMDC connected databases such as the Cologne database for molecular spectroscopy (CDMS), the jet propulsion laboratory molecular spectroscopy database (JPL), and the high-resolution transmission molecular absorption database (HITRAN).

Key words. molecular data – molecular processes – astronomical databases : miscellaneous – ISM :astrochemistry – standards

1. Introduction

The paper presents the scientific content of the BASECOL2023 edition [1]. BASECOL provides state-to-state inelastic atomic and molecular collisional rate coefficients with energy transfer in both the target and the projectile, in a temperature range suitable for radiative transfer modelling in the interstellar medium (ISM) or circumstellar atmospheres and cometary atmospheres, where local thermodynamic equilibrium (LTE) conditions are not fulfilled. In addition, the BASECOL format provides effective and thermalised rate coefficients, as stated below (Section 2.4). BASECOL provides a wide overview of the field of rate coefficient calculations for the above applications, and it follows the VAMDC standards (Albert et al. 2020; Dubernet et al. 2016). BASECOL is therefore accessible from VAMDC applications such as the VAMDC portal [2], the species database service [3], and other user tools that use VAMDC standards. One of the tools is the SPECTCOL tool [4] , the latest edition of which will be published in 2024.

Other databases, such as the Leiden atomic and molecular database (LAMDA) (van der Tak et al. 2020a) [5] and the excitation of molecules and atoms for astrophysics database (EMAA) [6], provide ready-to-use ASCII data files that combine selected rate coefficients and spectroscopic datasets. EMAA in particular allows the user to select the projectile(s) of interest, and a digital object identifier (DOI) is provided as a persistent identifier for each dataset.

Contents of the BASECOL2012 edition (Dubernet et al. 2013) were created by the scientific maintainer using rate coefficients mostly extracted from the literature. It was recently underlined by Dubernet et al. (2023) that this method is no longer sustainable. Therefore, the producers of rate coefficients are now invited to send their data formatted in a requested template. The current scientific content of the BASECOL database, called BASECOL2023, corresponds to the efforts of the various co-authors in providing their data with that template; in doing so, they contribute to the long-term preservation of the data and to the data indexation with relevant and community standard metadata for atomic and molecular data, that is VAMDC standards (Albert et al. 2020; Dubernet et al. 2016; Dubernet et al. 2010) [7]. From surveys of the literature, we know that there

⋆ marie-lise.dubernet@observatoiredeparis.obspm.fr
⋆⋆ otonieldenisalpizar@gmail.com
[1] https://basecol.vamdc.org
[2] https://portal.vamdc.eu
[3] https://species.vamdc.eu
[4] https://vamdc.org/activities/research/software/spectcol/
[5] https://home.strw.leidenuniv.nl/~moldata/
[6] https://emaa.osug.fr
[7] https://vamdc.org/activities/research/documents/standards/

are still missing rate coefficient datasets, and producers are welcome to contact the next BASECOL scientific leader, Dr Otoniel Denis-Alpizar, in order to include their data.

We would like to emphasise that BASECOL2023 provides an environment where the numerical data are not manipulated prior to their ingestion in the database, and if inconsistencies are noticed, the producers of the data are invited to provide new numerical data. In addition, prior to public access, the producers of the data privately visualise the display of their numerical and text data, and can ask that the BASECOL maintainer changes the text data. Finally, the references to the main papers for both the rate coefficients and the potential energy surfaces are provided, and the BASECOL home page emphasises that users must cite the original papers. The BASECOL technical design has been entirely updated: in particular, a versioning feature that allows accessibility to all versions has been added, and the dataset ingestion procedure has been reviewed in order to directly include the VAMDC metadata and to check the consistency of the datasets. A full description of the new BASECOL technical infrastructure is provided in Ba et al. (2020). From a scientific point of view, BASECOL2023 has been intensively updated in the past three years, and this paper provides the current status. BASECOL2023 contains a total of 491 collisional datasets of which 358 datasets correspond to the last version of the recommended datasets. It includes information on the collisional inelastic de-excitation of 103 atomic and molecular, neutral, and ionic species colliding mainly with projectiles such as H, He, H_2, and H_2O.

2. Description of the datasets found in BASECOL

2.1. Composition and display of datasets

The BASECOL data are organised and displayed in a collisional dataset. A dataset corresponds to a collision between two colliding species: the target and the projectile species. As the product species are formally the same as the colliding species (target and the projectile), BASECOL can handle elastic, inelastic, and possibly rearrangement processes if the product species are the same as the colliding species.

The species can either be neutral or charged and atomic or molecular in nature. It is described by its usual chemical formula and is internally uniquely identified by its InchIkey and InchI number [8], possibly supplemented by the nuclear spin symmetry (ortho, para, meta, etc.). The species database website [9] makes it possible to find the VAMDC species including the InchIkey and InchI number expressions.

Once the colliding species are identified, a dataset corresponds to three numerical tables: one table containing the process rate coefficients of the state-to-state energy level transitions of the two colliding species (in cm^3s^{-1}) as a function of temperature (in kelvin), and one table per species containing the energy levels whose labels characterise the transitions in the rate coefficient table (see Section 2.4 for the specific issues of labelling the energy levels transitions for effective and thermalised rate coefficients).

The unique dataset is associated with its 'main' publication, that is, the one in which it was published [10], and it is complemented by a short description of the methodologies used in the potential energy surface (PES) and the dynamical calculations wherever relevant. The PES's references are systematically cited, as well as references linked to the energy levels (for the latter it depends on the availability of the information provided by the data producer). Additional references -such as references linked to methodologies or to a historical review of the collisional system- that might be associated with the dataset are also cited. Additional information about precision or review of data is sometimes included. In particular, datasets are labelled as 'outdated' whenever this is the case, or are labelled 'not recommended' when the datasets have errors either mentioned in a published erratum or mentioned privately by the authors.

As part of the newly designed BASECOL structure (Ba et al. 2020), the versioning of the dataset has been introduced. A new version is created when the rate coefficient table and/or the associated energy table are changed, and BASECOL provides access to the previous versions of the datasets in order to guarantee traceability of data and reproducibility of usage. We comment on the modifications between versions.

2.2. Discussion on BASECOL recommendation

The BASECOL interfaces, which display the list of available datasets corresponding to a query, indicate the status, 'Recommended : yes or no'. 'Recommended : no' corresponds both to outdated datasets and to datasets with errors (see previous paragraph). It should be noted that VAMDC accesses the last version of the recommended datasets only to avoid confusing users. The current choice of BASECOL2023 is to provide access to 'recommended sets' only, but this paragdim could be changed upon a user's request.

A priori, all datasets are recommended when they are first included in the BASECOL database. The outdated datasets are 'non-recommended' for the following reasons: 1) new calculations are performed with a clearly more sophisticated potential energy surface, 2) new calculations are performed with more sophisticated scattering methodologies (e.g. the basis set is larger, the scattering method has less approximation). Nevertheless, some datasets are still recommended even if they do not fit the above criteria, as they offer alternative realistic datasets that can be used to test the influence of rate coefficients in radiative transfer studies.

The detailed description of the datasets given in the following paragraphs explain the choices.

2.3. BASECOL2023 molecular quantum number description

The description of BASECOL2023 quantum numbers follows the VAMDC standards [11]. Within VAMDC standards the molecules are classified by fourteen so-called cases [12]. Each case corresponds to a specific type of molecule: diatomic, linear triatomic, non-linear triatomic, linear polyatomic, symmetric top, spherical, and asymmetric molecules, combined with its electronic state separated into closed-shell and open-shell states. Diatomic open-shell molecules can be described in two possible cases: hunda (Hund's a coupling) and hundb (Hund's b coupling). Table A1 indicates the BASECOL2023 molecules and their cases.

Currently, three molecules have issues with the VAMDC cases because the energy tables provided by the authors cannot be described with the current VAMDC cases. The hundb case has been assigned to the C_4 ($X^3\Sigma_g^-$) energy table (ID=127) because the SpinComponentLabel label does not exist in the linear

[8] https://iupac.org/who-we-are/divisions/division-details/inchi/

[9] https://species.vamdc.eu

[10] The main publication is marked in red

[11] https://standards.vamdc.eu/#data-model

[12] https://amdis.iaea.org/cbc/

polyatomic open shell (lpos) case. The hunda has been assigned to the C_6H ($X^2\Pi$) energy tables (ID=154, 155) because the authors used (J,Ω) quantum numbers and the lpos case does not include Ω. This is a temporary solution while the VAMDC standards evolve. The CH_3OH molecule is described with a spherical top closed shell (stcs) case, in which the label rovibSym is used for the symmetry of the torsional function (see Sect. 9.9 for more information).

2.4. Rate coefficients

The collisional rate coefficients provided by BASECOL are state-to-state rate coefficients, effective rate coefficients, and thermalised rate coefficients, each of which is defined below. In most cases, state-to-state (de-)excitation rate coefficients ($R(T)$) are obtained at a given temperature from Boltzmann thermal averages of the calculated state-to-state inelastic cross-sections obtained on a grid of kinetic energies E:

$$R(\alpha \rightarrow \alpha';\beta \rightarrow \beta')(T) = \left(\frac{8}{\pi\mu}\right)^{1/2} \frac{1}{(k_B T)^{3/2}} \int_0^\infty \sigma_{\alpha\rightarrow\alpha';\beta\rightarrow\beta'}(E)\, E\, \mathrm{e}^{-E/k_B T}\, \mathrm{d}E, \quad (1)$$

where k_B is the Boltzmann constant, μ is the reduced mass of the colliding system, and (α,β), (α',β') represent the initial and final levels of the target (α) and projectile (β). Therefore, a typical BASECOL rate coefficient table is composed of the following items: columns 1 and 2 contain the initial α and final α' levels of the target, columns 3 and 4 contain the initial β and final β' levels of the projectile, the subsequent columns give the state-to-state rate coefficients (Eq. 1) at different temperatures (in kelvin).

These state-to-state collisional rate coefficients follow the principle of detailed balance, and reverse rate coefficients $R(\alpha' \rightarrow \alpha;\beta' \rightarrow \beta)(T)$ can be obtained from forward rate coefficients by the usual formula:

$$g_{\alpha'}\, g_{\beta'}\, \mathrm{e}^{-\frac{E'_{int}(\alpha')}{k_B T}}\, \mathrm{e}^{-\frac{E'_{int}(\beta')}{k_B T}} R(\alpha' \rightarrow \alpha;\beta' \rightarrow \beta) = g_\alpha\, g_\beta\, \mathrm{e}^{-\frac{E_{int}(\alpha)}{k_B T}}\, \mathrm{e}^{-\frac{E_{int}(\beta)}{k_B T}} R(\alpha \rightarrow \alpha';\beta \rightarrow \beta'), \quad (2)$$

where g_α and g_β are the statistical weights related to the ro-vibrational levels of the target and projectile, respectively, and the different E_{int} are the ro-vibrational energies of the species. When the projectile is an electron or an atom whose internal energy does not change during the collision, the state-to-state (de)-excitation rate coefficient is Eq. (1) with $\beta = \beta' = 1$.

When the projectile is a molecule, such as H_2 or H_2O, transitions are possible in the projectile molecule. Nevertheless, most published calculations with H_2 do not allow excitation of H_2, thereby fixing H_2 in its lowest para (-p) ($j = 0$) and ortho (-o) ($j = 1$) states. Within this approximation, the state-to-state (de)-excitation rate coefficient is Eq. (1) with $\beta = \beta' = 1$, similarly to atoms.

BASECOL allows the inclusion of the so-called effective rate coefficients $\hat{R}_\beta(\alpha \rightarrow \alpha')$ that are given by the sum of the state-to-state rate coefficients (Eq. 1) over final projectile states, β' for a given initial β:

$$\hat{R}_\beta(\alpha \rightarrow \alpha')(T) = \sum_{\beta'} R(\alpha \rightarrow \alpha';\beta \rightarrow \beta')(T). \quad (3)$$

In BASECOL the effective rate coefficients are identified as 'effective' in the title of the dataset, and the table's entry for the projectile initial level indicates the β level of Eq. (3), while the projectile's final level is meaningless and is currently set equal to the initial level for convenience. It should be mentioned that these effective rate coefficients do not follow the principle of detailed balance, so both excitation and de-excitation rate coefficients should be calculated explicitly.

Finally, thermalised de-excitation rate coefficients can be obtained by averaging over the initial ro-vibrational levels of the projectile:

$$\overline{R}(\alpha \rightarrow \alpha')(T) = \sum_\beta \rho(\beta) \hat{R}_\beta(\alpha \rightarrow \alpha')(T), \quad (4)$$

with $\rho(\beta) = g_\beta e^{-\frac{E_{int}(\beta)}{k_B T}}/Z(T)$, where $Z(T)$ is the partition function obtained as a sum over the β states. Such rate coefficients follow the principle of detailed balance automatically if an accurate quantum scattering methodology -such as the close-coupling (CC) or coupled states (CS) method- is employed. If the approximate scattering methodology is employed (such as classical, semi-classical, or mixed quantum/classical), the values of computed rate coefficients for excitation and quenching may need to be 'symmetrised' first to ensure that they satisfy the principle of detailed balance. The examples of such a symmetrisation procedure can be found in Boursier et al. (2020) and Mandal & Babikov (2023a).

For projectiles with ortho and para species such as H_2 or H_2O, the datasets can be calculated considering the two nuclear symmetries as independent. For example, the quasi-classical calculations (QCT) calculations by Faure et al. (2007b) directly calculate the rotational de-excitation rate coefficients of H_2O by thermalised ortho and para H_2 considered as separate species (labelled o/p-t-H_2 in the tables of the annex). Another example is the quantum de-excitation of HCN by a thermalised para-H_2O dataset (Dubernet & Quintas-Sánchez 2019) (labelled p-t-H_2O in the tables of the annex).

In some cases, the calculations are provided for a thermalisation over both the para- and ortho-projectile species. An example is the ro-vibrational de-excitation (Faure & Josselin 2008) of o/p-H_2O with thermalised H_2 over the two nuclear species (labelled t-H_2 in the tables of the annex) and the calculations for the de-excitation of o/p-H_2O by H_2O (Boursier et al. 2020; Mandal & Babikov 2023a) thermalised over both para- and ortho-H_2O projectiles (labelled t-H_2O in the tables of the annex). The user is referred to the papers to see how the thermalisation was performed.

In BASECOL, the thermalised rate coefficients are identified as thermalised in the title of the dataset, and the entries for the projectile's initial and final levels are meaningless. They are always denoted as the $\beta = \beta' = 1$ level for convenience.

2.5. Fitting information of the datasets

BASECOL2012 had fitting features that made it possible to download and to visualise fitting functions for rate coefficient datasets; those fits were either provided in the authors publications (mainly for electron impact collisions), or were mostly calculated by one of the former BASECOL maintainers (F. Daniel) for collisions with the heavy projectiles. The list of fitted datasets is indicated in Table A1 of our previous publication (Dubernet et al. 2013).

No additional set has been fitted since 2013 as the astrophysical users prefer to use their own fitting functions, but BASECOL2023 has been upgraded with a new graphical display of fits that allows us to visualise the quality of the fits.

The electron impact rate coefficients for D_2O, H_2O, and HDO datasets (Faure et al. 2004); HCN, HNC, DCN, and DNC

datasets (Faure et al. 2007b); SiO (Varambhia et al. 2009); the HC_3N–p-H_2 dataset (Wernli et al. 2007a,b); and the o-H_2CO–o/p-H_2 datasets (Troscompt et al. 2009) use the following fitting equation introduced by Balakrishnan et al. (1999a):

$$\log(R(T)) = \sum_{k=0}^{4} a_k \left[\frac{1}{T^{(1/6)}}\right]^k, \quad (5)$$

where $R(T)$ is the rate coefficient in cm^3s^{-1}, T the temperature in kelvin, and a_k the fitted coefficients.

The electron impact rate coefficients for the CO^+, HCO^+, NO^+, o/p-H_2^+ (Faure & Tennyson 2001), o/p-H_3^+, and o/p-H_3O^+ datasets (Faure & Tennyson 2003) used the following fitting function with $T_0 = 300K$:

$$\log(R(T)) = a \left[\frac{T}{T_0}\right]^b \exp(-c/T), \quad (6)$$

where $R(T)$ is the rate coefficient in cm^3s^{-1}, T the temperature in kelvin, and a, b, c the fitted coefficients. The electron-H_2^+ rate coefficients dataset of Sarpal & Tennyson (1993) is fitted with the latter formula where $T_0 = 1K$ (in BASECOL we used $\exp(c/T)$, so the coefficient c is negative for that particular dataset). The dataset (Lim et al. 1999) for the collision of CH^+ with electrons is fitted with

$$\log(R(T)) = a\ [T]^{[b+c\ln(T)]}, \quad (7)$$

where $R(T)$ is the rate coefficient in cm^3s^{-1}, T is the temperature in kelvin, and a, b, c are the fitted coefficients.

Apart from the above cited datasets, BASECOL2012 datasets for collisions with heavy projectiles have been internally fitted with the so-called common fit equation' (please note that there was a typo in the formula for this equation in Ba et al. (2020), which is corrected below):

$$\log(R(T)) = \sum_{k=1}^{N-1} a_k \left[\log\left(\frac{T}{\epsilon T_0}\right)\right]^{k-1} + a_N \left(\frac{1}{\frac{T}{\epsilon T_0} + \epsilon} - 1\right), \quad (8)$$

where $R(T)$ is the rate coefficient in cm^3s^{-1}, T is the temperature in kelvin, and ϵ, a_k are the fitted coefficients (in addition $T_0 = 1K$ is formally introduced for homogeneity purposes).

2.6. Search for the datasets

The search feature has evolved since the description of Ba et al. (2020). The 'collision' search of Ba et al. (2020) has been renamed 'browse collision', and a 'search collision' has been added. The latter search requires clicking on the fields in order to perform the selection, as can be seen in Fig. 1. This search collisions interface is extremely useful for rapidly querying the content of the database as one can access all datasets for a single or several target species, or for a single or several projectile species. One can find all datasets related to a given collisional process (rotation, vibration, ro-vibration, fine, and hyperfine). One can select a given range of years, the name of an author, or part of the name of an author. The implicit rule of selection between the year, target, target symmetry, collider (i.e. projectile), and collider symmetry (i.e. projectile symmetry) fields is an 'and' rule, and the explicit rule for a given field is an 'or' rule.

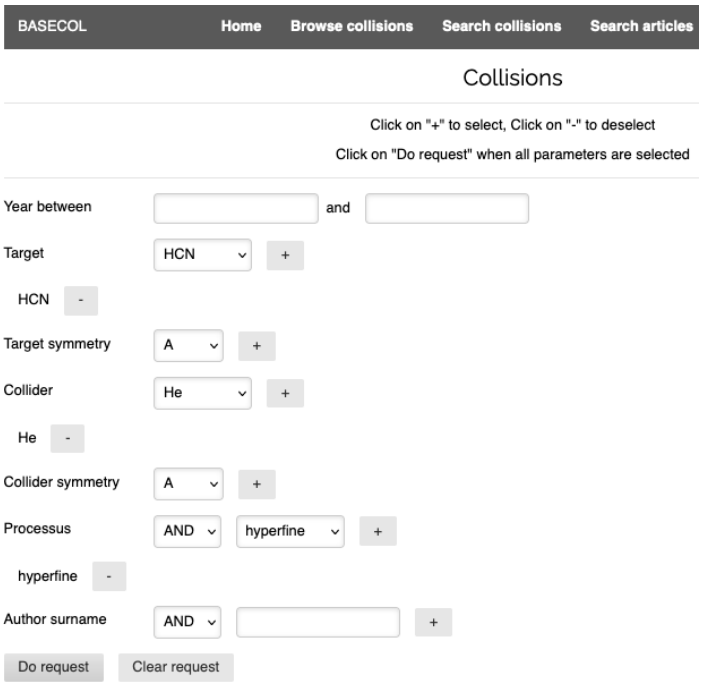

Fig. 1. Query interface for collisional rate coefficients for HCN-He with hyperfine selection. This interface is accessible from the 'search collisions' item in the black band

3. Bibliographic database

The 2023 bibliographic database can be independently searched in the search articles section (see Fig. 1). The bibliographic database includes the references attached to the collisional datasets only. The references are classified in five categories: category 1 corresponds to the main publication where the data are published, category 2 corresponds to the references of the potential energy surfaces used to calculate the rate coefficients, category 3 corresponds to references linked to the spectroscopy of the molecules (energy tables), category 4 is used whenever a methodology or a code is mentioned, and category 5 corresponds to the context. This category index selects which references are sent to VAMDC. Currently, we transfer all references up to and including category 3.

Each reference is indexed with keywords that allow us to narrow the search of references in the database, for example with respect to the target or projectile species, the type of data that can be found (cross-sections, rate coefficients, potential energy surfaces), the type of transitions (rotation, fine, hyperfine, etc.), or even the programs used (this can be found via the key term miscellaneous: program). The outputs of the bibliographic database are in BibTeX and in BASECOL internal format.

4. BASECOL policies

When the data producer submits the paper related to the datasets to a journal, he/she should contact the BASECOL scientific leader whose credentials are in the contact section of the BASECOL website. In return, the data producer receives the instructions and a directory containing examples of the files to be sent. We prefer not to provide the information online as items might change over time, and we stress the importance of following the instructions in order to speed up the procedure. Once the publication is accepted by a journal, the data producer sends the package of information that includes numerical data and text

data. The numerical data are composed of the rate coefficients table and the energy table that allows to identify the transitions in the rate coefficients table. To this effect, the producer is invited to follow VAMDC standards for the quantum numbers' designation. The text data are composed of a description of the main features of the methodology used in the calculations and a file containing the references cited in the methodology. The producer includes the relevant publications linked to the dataset in the package. The text data, references, energy table values, and additional metadata are included in the original producers' file, which contains the numerical values of the rate coefficients, and a so-called ingestion file is created. The BASECOL manager uploads this ingestion file to the database through a script that parses the file. The parsing procedure checks the consistency of the numerical data. Many items related to the structure of the ingestion file and to the ingestion procedure are already described in the BASECOL technical paper by Ba et al. (2020). During the process of creating the entries for BASECOL, the scientific maintainer interacts with the producer in order to verify any issues that might be raised in the various data. At the end, the producer verifies the data on a password-protected private website and gives his/her agreement for publication on the public website. From 2021 the BASECOL business model relies on the data producers sending data to the maintainer and following the above described policies. The data producer is informed and agrees that his/her mail credentials are kept so that the person who prepared the initial numerical data can be contacted.

5. Collisions with electrons

Table B1 provides the collisional systems with electrons as projectiles; no new dataset has been added since BASECOL2012, indeed no authors sent their data in the requested format. BASECOL2023 datasets have been upgraded with VAMDC standards for the description of quantum numbers, and the energy levels unit has been changed to wavenumbers whenever it was necessary. The electron impact rate coefficients are labelled 'recommended' in BASECOL, even if newer datasets can be found in the literature. For more recent information on electron impact collision for astrophysical applications, a review can be found in Tennyson & Faure (2019). In addition, several academic and open science databases, mainly aimed at plasma application, contain rate coefficients for the collisional excitation of atoms and molecules by electrons (see VAMDC (Albert et al. 2020) and the LAMDA (van der Tak et al. 2020a) [13] and EMAA [14] databases for astrophysical applications).

6. Atoms and atomic ions with heavy partners (H, He, o/p-H_2)

Table B2 provides the list of datasets for the excitation of the fine structure of C and C^+ (sometimes referred to as CI and C II, respectively), of O (OI), of S (S I), and of Si and Si^+ (SiI and Si II, respectively). We say that an atomic species has a complete collisional panel when datasets are available for the four projectiles: H, He, o/p-H_2.

The carbon atom C has a complete collisional panel. BASECOL2023 has been updated with a dataset (Bergeat et al. 2018) for the de-excitation of $C(^3P_J)$ by He for temperatures up to 350K. We consider that this dataset supersedes the dataset by Staemmler & Flower (1991) as the theoretical cross-sections reproduce most of the resonances found in the experimental results well; thus, we assume that the theoretical potential energy surfaces (PES) are accurate enough to provide reliable cross-sections and rate coefficients. BASECOL2012 already included the dataset from Abrahamsson et al. (2007) for $C(^3P_J)$ in collision with H that superseded the non-recommended dataset of Launay & Roueff (1977) and a dataset (Schröder et al. 1991) for $C(^3P_J)$ impacted by o/p-H_2 for temperatures up to 1000K/1200K.

The carbon $C^+(^2P_{1/2})$ ion has an incomplete collisional panel. The dataset $C^+(^2P_{1/2})$–H comes from Barinovs et al. (2005) for temperatures up to T=2000K. BASECOL2023 has been updated with two datasets (Kłos et al. 2020a) for the quenching of the spin-orbit transition of $C^+(^2P_{1/2})$ by o/p-H_2 for temperature up to 500K; those datasets have been calculated with a newly calculated PES (Kłos et al. 2020a) and with CC calculations using a basis set that includes rotational levels of ortho-H_2 up to j=15 or of para-H_2 up to j=16. The dataset with ortho-H_2 corresponds to state-to-state rate coefficients restrained to o-H_2 remaining in its lowest rotational level (j=1), while the dataset for para-H_2 corresponds to thermalised rate coefficients (see Eq. 4) calculated with state-to-state rate coefficients involving transitions between para-H_2 rotational levels.

The oxygen atom $O(^3P_J)$ has a complete collisional panel. The quenching of the spin-orbit transition of $O(^3P_J)$ by H has been revisited by two groups (Lique et al. 2017; Vieira & Krems 2017), and new calculations for the de-excitation of $O(^3P_J)$ by o/p-H_2(Lique et al. 2017) and by He (Lique et al. 2017) have been performed. BASECOL2023 has been updated with these five recommended datasets. Therefore, the old datasets for O–H (Abrahamsson et al. 2007; Launay & Roueff 1977) and O–o/p-H_2(Jaquet et al. 1992) are now obsolete and labelled as non-recommended.

For the quenching of the oxygen atom $O(^3P_J)$ by H, the competing datasets (Lique et al. 2017; Vieira & Krems 2017) calculated the same year, use different potential energy surfaces, but identical spin-coupling terms (Parlant & Yarkony 1999): the calculation of Lique et al. (2017) uses the recent PES from Dagdigian et al. (2016), and the calculations of Vieira & Krems (2017) use the PES from Parlant & Yarkony (1999). Vieira & Krems (2017) mentioned that they corrected some errors made by Abrahamsson et al. (2007), and with the help of machine learning techniques they provide error bars on the rate coefficients.

For the S (^{3}P), Si (^{3}P) atoms and the $Si^+(^2P_{1/2})$ ion, the collisional panel is incomplete since only one projectile is available: either H or He. The dataset (Barinovs et al. 2005) for the quenching of the spin-orbit transition of Si^+ by H for temperatures up to 2000K was already in BASECOL2012. BASECOL2023 has been updated with two recent datasets (Lique et al. 2018) for the de-excitation of S (^{3}P) by He and of Si (^{3}P) by He for temperatures up to 1000K.

7. Diatomic molecules with heavy partners.

The diatomic species table B3 includes neutral molecules, cations and anions in collision with He, H and H_2 for astrophysical applications, as well as some collisional datasets concerning excitation by Ar and Ne.

7.1. Anions and cations

BASECOL2012 had three ionised species only. It included the rotational de-excitation of CH^+ by He with two recommended

[13] https://home.strw.leidenuniv.nl/~moldata/
[14] https://emaa.osug.fr

datasets: one dataset (Turpin et al. 2010) for transitions among six rotational levels (T=1-200K) and another dataset (Hammami et al. 2009) for transitions among 11 levels (T=20-2000K). The latter dataset already superseded an older dataset (Hammami et al. 2008a) marked as non-recommended. BASECOL2012 also included the rotational de-excitation among eleven rotational levels of CN^- by o/p-H_2 (Kłos & Lique 2011) and among eleven levels of SiH^+ by He (Nkem et al. 2009). BASECOL2023 has been updated with nine additional datasets concerning the rotational and vibrational excitation of C_2^- (Mant et al. 2020a,c,b) in collision with He, Ar, and Ne, and of CN^- (González-Sánchez et al. 2020; González-Sánchez et al. 2021; Mant et al. 2021) in collision with He and Ar. As far as cations are concerned, the new additions mainly concern rotational de-excitation of the following species: AlO^+ by He (Denis-Alpizar et al. 2018c); $^{36}ArH^+$ by He (Bop et al. 2016); $^{36}ArD^+$ by He (García-Vázquez et al. 2019); CF^+ by He (Denis-Alpizar et al. 2018a), by p-H_2 (Denis-Alpizar & Rubayo-Soneira 2019; Desrousseaux et al. 2021), and by o-H_2 (Desrousseaux et al. 2021); HeH^+ by H (Desrousseaux & Lique 2020); NeH^+ by He (Bop et al. 2017); NO^+ by He (Denis-Alpizar & Stoecklin 2015) and by p-H_2 (Cabrera-González et al. 2020); and NS^+ by He (Cabrera-González et al. 2018).

In the case of the collisional rotational excitation of CF^+ with p-H_2 (Denis-Alpizar & Rubayo-Soneira 2019; Desrousseaux et al. 2021), a good agreement was found between the two new sets of data despite the use of a less accurate PES by Denis-Alpizar & Rubayo-Soneira (2019). The dataset of Denis-Alpizar & Rubayo-Soneira (2019) provides rate coefficients for roughly the same transitions, but for temperatures between T=10K and T=300K, while Desrousseaux et al. (2021) provides data between T=5K and T=150K.

The de-excitation among rotational levels of NS^+ cation by H_2 has been included with several datasets: a first dataset (Bop 2019) (24 levels; T=5-100K) of NS^+ in collision with p-H_2 (j=0) that was calculated with a PES spherically averaged over the H_2 directions, and two datasets (Bop et al. 2022a) (15 levels; T=5-50K) in collision with p-H_2 (j = 0) and with o-H_2 (j = 1); both datasets were calculated with a 4D PES (Bop et al. 2022a). For these datasets, the authors (Bop et al. 2022a) performed some interesting precision tests related to the dimension of the H_2 rotational basis in the dynamical calculations. They found that the neglect of higher H_2 rotational levels induced differences up to 30% in the rate coefficients.

The rate coefficients among hyperfine levels, obtained via IOS recoupling techniques, are added for CF^+ by He (Denis-Alpizar et al. 2018a), for NS^+ by He (Cabrera-González et al. 2018), and for NS^+ by p-H_2(j = 0) (Bop 2019). The rovibrational excitation of $^{36}ArH^+$ by He (García-Vázquez et al. 2019) has been added as well.

7.2. CH

BASECOL2023 is enriched with the CH species with two datasets: the fine structure resolved excitation of $CH(^2\Pi)$ by He (Marinakis et al. 2015) and the hyperfine structure resolved excitation for $CH(^2\Pi)$–He (Marinakis et al. 2019). The hyperfine results are obtained with a recoupling technique using the data from Marinakis et al. (2015).

7.3. CN, ^{13}CN, C^{15}N

The current CN data (Table B3) include collisions with He and H_2 and tackle rotational, fine and hyperfine resolved de-excitation processes. Nine recommended datasets are available for CN, one for ^{13}CN and one for C^{15}N.

7.3.1. CN–He

BASECOL2012 included the CN-He system with two datasets: one for transitions among the lowest 41 fine levels of CN for temperatures between 5 and 350K (Lique et al. 2010b) and for transitions among the lowest 37 hyperfine levels of CN for temperatures between 5 and 30K (Lique & Kłos 2011).

7.3.2. CN and isotopologues with H_2

BASECOL2023 has been enriched with collisional processes involving the H_2 projectile for CN, ^{13}CN, and C^{15}N. The CN-H_2 saga includes a first publication by Kalugina et al. (2012), where they calculated a 4D PES and then reduced the dimensionality to a 3D PES in order to calculate rate coefficients among hyperfine levels of CN in collision with p-H_2(j=0). This dataset, included in BASECOL2012, is now superseded by the new calculations cited thereafter and marked as non-recommended. In a subsequent publication, Kalugina et al. (2013) calculated a 4D PES, and using this 4D PES they calculated rate coefficients among rotational and fine resolved structure of CN in collision with o-H_2 (j = 1) and with para-H_2 (j=0,2); for the fine resolved structure calculations they used a recoupling technique. For para-H_2 they provided state-to-state rate coefficients that include transitions $j(H_2)$ = 0-0, 2-2 and 2-0 (note that separate fine structure datasets are provided for $j(H_2)$ = 0-0 and $j(H_2)$ = 2-0, 2-2 as the 0-0 dataset includes 25 transitions among 25 fine levels of CN, while the $j(H_2)$ = 2-0, 2–2 datasets involve 17 fine levels). Finally, Kalugina & Lique (2015) used the PES from Kalugina et al. (2013) to calculate rate coefficients among hyperfine levels of CN using a recoupling technique. The hyperfine rates from (Kalugina & Lique 2015) are within a factor of two of those reported in (Kalugina et al. 2012) due primarily to the use of a reduced PES in the latter case. Two new datasets have been added for the hyperfine excitation of ^{13}CN and of C^{15}N by para-H_2 (Flower & Lique 2015), where the PES of Kalugina et al. (2013) is used.

7.4. CO

The current CO data (Table B3) include collisions with H, He, H_2, and H_2O, and tackle rotational, vibrational, and rovibrational de-excitation processes. 17 recommended datasets are available.

7.4.1. CO–He

BASECOL2012 already had datasets (Cecchi-Pestellini et al. 2002) for the de-excitation of 15 rotational levels of CO (T=5-500K) and of seven vibrational levels of CO (T=500-5000K).

7.4.2. CO–H

BASECOL2012 had a dataset by Balakrishnan et al. (2002) for the de-excitation of five vibrational levels of CO in the temperature range from 100K to 3000K. BASECOL2012 also in-

cluded two datasets (Balakrishnan et al. 2002) calculated with the CC method; they span the low-temperature range (T=5-100K) among eight rotational levels and the high-temperature range (T=100K-3000K) among 17 rotational levels. These three datasets were calculated with the PES of Keller et al. (1996); they are kept as recommended in order to provide meaningful comparisons with the more recent data cited below. New datasets for the CO-H system have been added to BASECOL2023 for rotational de-excitation (Walker et al. 2015) and for ro-vibrational de-excitation (Song et al. 2015b,a); both datasets use the PES of Song et al. (2013).

The rotational de-excitation rate coefficients (Walker et al. 2015) for temperatures ranging from 2K to 3000 K are obtained for CO (v = 0, j) quenching from j = 1-45 to all lower j' levels, where j is the rotational quantum number. CC and CS calculations were performed in full dimension for j = 1-5, 10, 15, 20, 25, 30, 35, 40, and 45, while scaling approaches were used to estimate rate coefficients for all other intermediate rotational states.

For the ro-vibrational de-excitation process in the temperature range from 2 to 3000 K, the dataset (Song et al. 2015b) provides the rate coefficients from initial states (v=1-5, j=0-30) to (v', j'), where v'= 0, 1, ..., v − 1, and j'=0, 1, ..., the highest final j' = 27 - 42, depending on the initial j. The transitions for larger final j' are not reported, either because they are negligibly small, or because they were not completely converged. It should be noted that the rate coefficients for ro-vibrational (v = 1, j = 0-30) → (v'=0, j') transitions were obtained from scattering cross-sections previously computed with the CC method by Song et al. (2015a). Combining these with the rate coefficients for vibrational v=1-5 → $v' < v$ quenching obtained with the infinite-order sudden approximation, Song et al. (2015b) used a extrapolation scheme that yields the rate coefficients for ro-vibrational v = 2-5, j=0-30, de-excitation.

7.4.3. CO–H_2

BASECOL2012 already contained datasets (Yang et al. 2010) calculated with the PES of Jankowski & Szalewicz (1998), which provided the rotational de-excitation of CO by o/p-H_2 among the lowest 41 rotational CO levels and for temperature between 1K and 3000K. The above datasets provide a larger number of transitions for a larger temperature range than previous datasets (Wernli et al. 2006; Flower 2001a) calculated with the same PES (Jankowski & Szalewicz 1998). All datasets are kept as recommended, as no strong argument can distinguish between the methodologies.

New datasets for the ro-vibrational de-excitation of CO by o/p-H_2 have been added to BASECOL2023 (Yang et al. 2016): the ro-vibrational de-excitation rate coefficients for all transitions from CO (v=1, j=1-5) to (v'=0, j'=0-22) in collisions with para-H_2 (j=0) and ortho-H_2 (j=1) are provided. In addition, the state to state rate coefficients for vibrational transitions of CO from (v=2, j=0) to (v'=1 and 0, j'=0-20) are also provided for para-H_2 remaining in its ground rotational state (j=0) and for para-H_2 excited from j=0 to j=2. Those calculations are based on the PES of Yang et al. (2015b).

7.4.4. CO–H_2O

For cometary applications, BASECOL2023 has been updated with two datasets (Faure et al. 2020) with thermalised rate coefficients for the de-excitation of CO by o/p-H_2O (11 levels; T=5-100K). The calculations use a new 5D PES (Kalugina et al. 2018) and the statistical approach of Loreau et al. (2018). The thermalised rate coefficients are obtained from the state-to-state rate coefficients summing over the final states of o/p-H_2O and averaging over the initial rotational states of o/p-H_2O where p-H_2O and o-H_2O are independent species.

7.5. CS

The CS data (Table B3) include collisions with He and H_2, and tackle rotational and ro-vibrational processes; six recommended datasets are available.

7.5.1. CS–He

BASECOL2012 already included collisions of CS with He that are still recommended: one dataset (Lique et al. 2006b) for the de-excitation among the lowest 31 rotational levels of CS (T=10K-300K) and another one (Lique & Spielfiedel 2007) for the de-excitation among the lowest 114 ro-vibrational levels (T=300-1500K).

7.5.2. CS–H_2

BASECOL2023 has been updated with collisional processes with the H_2 molecule. The recent rotational de-excitation datasets for CS by o/p-H_2 of Denis-Alpizar et al. (2018b) have been added and supersede previous results (Turner et al. 1992; Green & Chapman 1978) calculated with an old PES (Green & Chapman 1978).

Two new datasets by Yang et al. (2018a) have been included for the ro-vibrational de-excitation of CS by o/p-H_2. Those datasets cover the ro-vibrational de-excitation rate coefficients from the CS ro-vibrational states (v=1, j=1-5) to the (v'=0, j'=0-35) levels in collision with para-H_2 (j=0) and with ortho-H_2 (j=1). In addition, the state-to-state rate coefficients for ro-vibrational transitions of CS from (v=1, j=1-5) to (v'=0, j'=0-33) are also provided for para-H_2 excited from j=0 to j=2, as well as the state-to-state rate coefficients for ro-vibrational transitions of CS from (v=1, j=1-5) to (v'=0, j'=0-28) for ortho-H_2 excited from j=1 to j=3. Within those two datasets, the rotational de-excitation rate coefficients among the first six rotational levels of CS are also provided for v=0 for collisions with both para-H_2(j=0) and ortho-H_2(j=1).

7.6. HCl

The current HCl data (Table B3) include collisions with He, H_2, and H, and tackle rotational and hyperfine resolved de-excitation processes. Six recommended datasets are available.

7.6.1. HCl–He

BASECOL2023 has been updated with three datasets: two datasets for the de-excitation among rotational levels of HCl, those sets have been calculated by Lanza & Lique (2012) (11 levels; T=10-300K) and by Yang & Stancil (2014) (21 levels; T=1-3000K), and a dataset for the de-excitation from hyperfine resolved transitions (40 levels; T=10-300K) (Lanza & Lique 2012) obtained by a recoupling technique. The rotational datasets of Lanza & Lique (2012) and of Yang & Stancil (2014) are of comparable quality and are both recommended; in addition, the hyperfine rate coefficients could be obtained from the

latter dataset (Yang & Stancil 2014) using the usual recoupling techniques (Lanza & Lique 2012). These datasets supersede the previous rotational and hyperfine datasets of Neufeld & Green (1994) as Lanza & Lique (2012) and Yang & Stancil (2014) use more recent PES and better methodologies for the scattering calculations. The datasets of Neufeld & Green (1994) are now marked as non-recommended.

7.6.2. HCl–H_2

BASECOL2023 has been updated with two rotational datasets (Lanza et al. 2014a) for the de-excitation among the eleven lowest rotational levels of HCl (T=10-300K) with o/p-H_2. Those rotational state-to-state rate coefficients were obtained with rotational basis sets that include, respectively, the j_2=3 and j_2=2 levels of H_2. It should be mentioned that the dataset with para–H_2 includes transitions among the j_2=0,2 levels of H_2 projectile.

7.6.3. HCl–H

More recently, calculations including dissociation were performed by Lique & Faure (2017) for the rotational excitation of HCl-H system. Their rotational de-excitation rate coefficients (Lique & Faure 2017) (11 levels; T=10-500K) are now in BASECOL2023.

7.7. HF

The current HF data (Table B3) include collisions with He, H_2, H, and H_2O, and tackle rotational de-excitation processes. Seven recommended datasets are available.

7.7.1. HF–He

BASECOL2023 has been updated with a dataset (Yang et al. 2015a) for the rotational de-excitation of HF by He (21 levels and T=1-3000K), this dataset is calculated with the PES of Moszynski et al. (1994). BASECOL2012 already included the dataset Reese et al. (2005) (10 levels; T=0.1-300K) that was calculated with the more recent PES of Stoecklin et al. (2003). Yang et al. (2015a) presented a comparison with the results obtained by Reese et al. (2005); they indicate a percentage difference from 20% to 75% at 50K for most of the strongest transitions. As no objective quality arguments can be put forward, the two datasets are kept as recommended.

7.7.2. HF–H_2

BASECOL2023 has also been updated with two datasets (Guillon & Stoecklin 2012) for the de-excitation of six rotational levels of HF in collision with o/p-H_2 (T=0.1 - 150K): these datasets include some transitions within the H_2 rotational levels.

7.7.3. HF–H

A recent dataset (Desrousseaux & Lique 2018) for the rotational de-excitation of HF by H (9 levels T=10-500K) has been added to BASECOL2023; it uses the PES of Li et al. (2007).

7.7.4. HF–H_2O

For cometary applications, BASECOL2023 has been updated with two datasets (Loreau et al. 2022) with thermalised rate coefficients for the de-excitation of HF by o/p-H_2O (7 levels; T=5-150K). The calculations use a new 5D PES (Loreau et al. 2020) and the statistical approach of Loreau et al. (2018). The thermalised rate coefficients are obtained from the state-to-state rate coefficients summing over the final states of o/p-H_2O and averaging over the initial rotational states of o/p-H_2O where p-H_2O and o-H_2O are independent species.

7.8. HD

The current HD data (Table B3) include collisions with He, H_2, and H, and tackle rotational and ro-vibrational de-excitation processes. Ten recommended datasets are available.

7.8.1. HD–He

All the BASECOL datasets concerning HD in collision with He had been calculated using the PES of Muchnick & Russek (1994). BASECOL2012 already had the rotational de-excitation of HD by He (10 levels; T=80-2000K) by Roueff & Zeippen (1999). BASECOL2023 has been updated with two datasets from Nolte et al. (2011) for the ro-vibrational de-excitation of HD by He: those two datasets span different temperature range and transitions. In those calculations, Nolte et al. (2011) extended the calculations of Roueff & Zeippen (2000) to include transitions with j=0 and 1 for v= 0-17, and for which Δv =0,-1, -2. Compared to Roueff & Zeippen (2000), significant discrepancies were found for the highest previously considered vibrational state of v = 3, but for v=0, 1, 2, the new results are very close to previous results. The ro-vibrational data from Roueff & Zeippen (2000) were never provided to BASECOL.

7.8.2. HD with H_2 projectile

Two new datasets, calculated with the PES of Patkowski et al. (2008), have been included in BASECOL2023 for the de-excitation of nine rotational levels of HD by o/p-H_2 (Wan et al. 2019) for temperatures up to 10000K. These results supersede the results of Flower (1999a) (9 levels; T=50-500K) as the latter calculations used on older PES (Schwenke 1988) and did not take into account the excitation of the H_2 molecule in the rotational basis set. Therefore, the rotational dataset from Flower (1999a) is now indicated as non-recommended. The BASECOL2012 datasets for the ro-vibrational de-excitation of HD by o/p–H_2 by Flower & Roueff (1999a) with the PES of Schwenke (1988) have not been revisited and to our knowledge are currently the only available datasets.

7.8.3. HD–H

A new dataset for the rotational de-excitation of eleven rotational levels of HD by H (Desrousseaux et al. 2018) was added to BASECOL2023 in the temperature range between 10K and 1000K; calculations were performed with the PES of Mielke et al. (2002). BASECOL2012 already included the rotational de-excitation of HD by H for ten rotational levels and a temperature range from 100K to 2000K (Roueff & Flower 1999) where the PES of Boothroyd et al. (1996) was used. The rotational dataset of Roueff & Flower (1999) is kept as recommended to keep the coherence with the ro-vibrational de-excitation rate coefficients

of HD by H (Flower & Roueff 1999a) calculated with the same PES (Boothroyd et al. 1996). In addition, there is no strong argument about the difference of quality of the PES of Boothroyd et al. (1996) and the one of Mielke et al. (2002).

7.9. H_2

The current H_2 data (Table B3) include collisions with He, H_2, and H, and they tackle rotational and ro-vibrational de-excitation processes. Eleven recommended datasets are available.

BASECOL2023 was updated with one new dataset for the collision of H_2 with H (Lique et al. 2012), where the ortho-para conversion was tackled. All the other datasets were already included in BASECOL2012, and they form a very complete manifold of datasets calculated at the end of the last century.

7.9.1. H_2 with He projectile

The ro-vibrational de-excitation datasets of o/p-H_2 by He calculated with the PES of Muchnick & Russek (1994) are currently the only available datasets (Flower et al. 1998) in BASECOL. These results can be used for the rotational de-excitation of o/p-H_2 by He. Flower et al. (1998) provided ro-vibrational rate coefficients for all transitions among levels below (v=3, j ≤ 8, E=15228.88 cm^{-1}) for para-H_2 and below (v=3, j ≤ 7, E=14495.46 cm^{-1}) for ortho-H_2 (T=100K-6000K). It should be noted that for para-H_2 the rate coefficients had not been calculated for transitions involving the 27th level of para-H_2, (i.e. v=1, j=14), but they were available for transitions involving the 28th level (v=3, j=8); so, in BASECOL2023 we decided to limit the data set at the 26th level. For ortho-H_2, the rate coefficients had not been calculated for transitions involving level 24 (i.e. v=2, j=11), but they were calculated for transitions involving level 25 (v=3, j=7), so in BASECOL2023 we limited the dataset at level 23. In BASECOL2012, the rate coefficients for the missing transitions were set to zero. Nevertheless, another work has been carried out for this system. Balakrishnan et al. (1999b) calculated ro-vibrational de-excitation rate coefficients from v=2 to 6, with Δv=-1, for temperatures between 100K and 4000K. For ortho-H_2 the transitions involve de-excitation from (v, j=1-7) to (v − 1, j=1-11) and to (v, j=1-5). For para-H_2 the transitions involve de-excitation from (v, j=0-6) to (v − 1, j=0-10) and to (v, j=0-4). These calculations are an extension for v=4, 5, 6 of the work of Flower et al. (1998) using the same PES (Muchnick & Russek 1994). It should be noted that the calculations of Balakrishnan et al. (1999b) are an extension of the calculations by Balakrishnan et al. (1999a), but with a larger ro-vibrational basis set. Ro-vibrational results of Balakrishnan et al. (1999b) and Flower et al. (1998) show discrepancies for ro-vibrational results with large Δ j transitions, but there is no conclusion about the respective quality of results. As far as pure rotational calculations are concerned, Flower et al. (1998) and Balakrishnan et al. (1999a) agree well at the published temperature (100K and higher). For unknown reasons, those data have never been included in BASECOL, and if the authors (Balakrishnan et al. 1999a) provide their data in the BASECOL format, we are happy to include them.

7.9.2. H_2 with o/p-H_2 projectile

BASECOL2023 includes four datasets (Flower & Roueff 1998a, 1999b) with the o/p-H_2 projectile; those datasets have been obtained with the PES of Schwenke (1988). With the p-H_2 projectile kept in its ground state (v=0, j=0), two datasets (Flower & Roueff 1998a) provide ro-vibrational rate coefficients between 100K and 6000K for the de-excitation from the 26 lowest target para-H_2 levels, and from the 23 lowest target ortho-H_2 levels. Flower & Roueff (1998a) calculated more levels: for para-H_2 such that $j \leq 16$ in v=0, $j \leq 12$ in v=1, and $j \leq 8$ in v=2 and for target ortho-H_2 levels such that $j \leq 15$ in v=0, $j \leq 13$ in v=1, $j \leq 9$ in v=2, and $j \leq 7$ in v=3. For the reasons developed above for H_2–He, BASECOL2023 truncates the datasets.

With the ortho-H_2 projectile kept in its ground state (v=0, j=1), two datasets (Flower & Roueff 1999b) provide ro-vibrational rate coefficients between 100K and 6000K for the de-excitation from the 19 lowest target para-H_2 levels, and from the 17 lowest target ortho-H_2 levels. Flower & Roueff (1999b) calculated ro-vibrational rate coefficients for more levels in the case of ortho-H_2 such that j ≤ 15 in v=0, $j \leq 13$ in v=1 and $j \leq 9$ in v=2. But rate coefficients have not been calculated for transitions involving the 18th and 20th levels of the ortho-H_2 target (i.e. v=3,j=1; v=3,j=3). Therefore, BASECOL2023 provides the data set up to level 17 of the ortho-H_2 target. We are aware of the recent calculations by Hernández et al. (2021) of rotational H_2-H_2 de-excitation rate coefficients and we invite the authors to provide the data in our format.

7.9.3. H_2 with H projectile

Currently, BASECOL2023 includes two datasets (Flower & Roueff 1998b) for the ro-vibrational de-excitation of o/p-H_2 by H; those datasets have been calculated with the PES of Boothroyd et al. (1996) and provide rate coefficients from 100K to 6000K: one dataset for p-H_2 with 26 ro-vibrational levels and another one for o-H_2 with 23 ro-vibrational levels (see the paragraph on H_2-He above for explanations on the number of levels in the datasets).

The above results could be used for the rotational excitation of o/p-H_2 by H, but the pure rotational rate coefficients have differences as much as a factor of 2 compared to the results of Forrey et al. (1997) and the contribution of the reactive channel to the inelastic rate coefficients is not included as been done in Lique et al. (2012).

BASECOL includes the two datasets calculated by Forrey et al. (1997) that provide rotational de-excitation among the lowest three rotational levels of either p-H_2 or o-H_2 between 100K and 1000K. These datasets have been calculated with the same 3D PES (Boothroyd et al. 1996) as the ro-vibrational datasets of Flower & Roueff (1998b), but an exact wave function for H_2 is used instead of a harmonic approximation. This approximation is likely to explain the difference of factor of two between the two types of calculations. Indeed, Forrey et al. (1997) compared various ways to reduce a 3D PES to a 2D PES: a rigid rotor approximation, an average of 3D PES over the harmonic oscillator approximation, an average of 3D PES over the exact ro-vibrational wave function. They found that the rigid rotor approximation and the harmonic oscillator wave function strongly underestimate the rotational cross-sections (about a factor of two).

Finally, the combination of inelastic scattering of H_2 by H and ortho-para conversion of H_2 via H exchange has been studied by Lique et al. (2012) using the PES of Mielke et al. (2002). BASECOL2023 has been updated with the corresponding dataset of collisional rate coefficients among the first nine rotational levels of H_2 in collision with H for temperatures between 300K and 1500K (Lique et al. 2012). The differences between the data-sets of Forrey et al. (1997), Flower & Roueff (1998b),

and Lique et al. (2012) are given in Figure C.1 and show the importance of considering the exchange channel for this collision.

7.10. KCl

BASECOL2023 was updated with the KCl molecule and with a single dataset (Sahnoun et al. 2018) concerning the de-excitation of KCl by p-H_2 (j=0) among the 16 lowest rotational levels of KCl (T=2-50K).

7.11. NaH

Another new molecule is NaH, and the current unique dataset (Bop et al. 2019b) concerns the rotational de-excitation of NaH by He (11 levels; T=5-200K) calculated with a PES averaged over the ground vibrational wave function of NaH (Bop et al. 2019b).

7.12. NH

The NH($X^3\Sigma^+$) data (Table B3) include collisions with He and tackle the rotational fine structure process; two recommended datasets are available, and no strong arguments could be used to distinguish between them. BASECOL2023 has been updated with a new dataset (Ramachandran et al. 2018) for the fine structure rotational excitation of NH by He (25 levels; T=10-350K). This dataset has been calculated with a 2D PES averaged over a 3D PES that included the vibrational coordinate of NH when the previous dataset of Toboła et al. (2011), already in BASECOL2012, had been calculated with a 2D PES. It should be noted that both datasets agree reasonably well with the experimental rate coefficients of Rinnenthal & Gericke (2002); they both provide transitions among the lowest 25 rotational levels and in the same temperature range up to 350K. Figure C.2 (see annex) displays the differences between the two calculated rate coefficient datasets: as it appears that they do not show any significant differences (the average percentage difference between the two data sets is less than 40% for the $\Delta N = \Delta F$ transition), and it is worth noting that the differences are not homogeneous. Both datasets are marked as recommended in BASECOL2023.

7.13. NO

The NO data (Table B3) include collisions with He and H_2 and tackle fine and hyperfine processes; two recommended datasets are available. BASECOL2012 already had the dataset (Kłos et al. 2008) for the rotational de-excitation of the fine structure levels of NO by He (98 levels; T=10-500K). On that dataset (Kłos et al. 2008), BASECOL2023 has updated the notation for the Kronig parity labels in order for them to agree with VAMDC standards, and the energy levels have been put in increasing order, but the scientific content is not changed; the final version of the dataset has changed to v4. BASECOL2023 has been updated with a dataset (Ben Khalifa & Loreau 2021) for the rotational de-excitation of the hyperfine structure of NO by p-H_2 (100 levels; T=7-100K), the authors use the new PES of Kłos et al. (2017a).

7.14. OH, OD

The OH data (Table B3) include collisions with He, H_2, and H, and tackle rotational fine and hyperfine structure resolved processes. Ten recommended datasets are available.

7.14.1. OH–He

The oldest dataset (Kłos et al. 2007), already in BASECOL2012, includes fine structure de-excitation rate coefficients of OH by He using the 2D PES of Lee et al. (2000). BASECOL2023 has been updated with a more recent dataset (Kalugina et al. 2014) that provides rate coefficients for the same system and process. This is for the same number of transitions (roughly 44) and for the same temperature range (T=5-350K), but the authors used the new vibrationally averaged 3D PES of Kalugina et al. (2014). The discussions of Kalugina et al. (2014) seem to show that a vibrationally averaged PES provides some theoretical results in closer agreement with the experimental results. Nevertheless, other tests (Kalugina et al. 2014) show no difference in using either a 2D or an averaged 3D PES. For all the above reasons, the two datasets are indicated as recommended. We checked both sets of rate coefficients at 5, 10, 50, and 300 K. For the transitions up to level 9.5e, the agreement is good, with averaged percentage differences of 28.3, 19, 18.4, and 10.9, respectively. However, for transitions from level 9.5e up to level 10.5e, the averaged percentage differences are 172.2, 130.1, 64.3, and 101, respectively.

BASECOL2023 is further updated with a dataset (Marinakis et al. 2019) that provides hyperfine resolved collisional de-excitation rate coefficients of OH by He. The authors used a recoupling technique together with the nuclear spin-free S matrices of Kalugina et al. (2014).

7.14.2. OH/OD–H_2

The OH–H_2 system has been investigated by Offer et al. (1994), the corresponding datasets can be found on the LAMDA database (van der Tak et al. 2020b). BASECOL2023 was updated with two datasets (Kłos et al. 2017b) for the fine structure de-excitation of OH by o/p-H_2 (20 levels; T=10-150K) and two datasets (Kłos et al. 2020b) for the hyperfine resolved structure de-excitation of OH by o/p-H_2 (24 levels; T=10-150K), the four datasets were obtained with the PES of Ma et al. (2014). The OH–H_2 fine structure rate coefficients for collisions with both para-H_2(j = 0) and ortho–H_2 (j = 1) differ by a factor of less than three from the older rates by Offer et al. (1994), and the new hyperfine resolved rate coefficients (Kłos et al. 2020b) are found to increase the hyperfine intensities by a factor of about 1–3 in comparison to previous rates of Offer et al. (1994). The new OH–H_2 rate coefficients (Kłos et al. 2017b, 2020b) are expected to be more precise than the previous ones (Offer et al. 1994), as the new datasets were obtained with the recent PES (Ma et al. 2014) that performed fairly well in comparison of theoretical calculations with scattering experiments (Schewe et al. 2015). The OD molecule is new in BASECOL, and two datasets (Dagdigian 2021a) provide hyperfine resolved structure de-excitation of OD by o/p-H_2 (40 levels; T=5-200K); they were obtained with the same PES (Ma et al. 2014) as above.

7.14.3. OH–H

BASECOL2023 was updated with a dataset (Dagdigian 2022a) that provides hyperfine resolved collisional de-excitation rate coefficients of OH by H atoms calculated with a recoupling technique and with fine resolved structure excitation results of OH by H (Dagdigian 2022b). These calculations used the potential energy curves of Alexander et al. (2004).

7.15. O_2

The O_2 data (Table B3) include collisions with He and o/p-H_2, and tackle rotational and fine structure resolved processes; three recommended datasets are available. BASECOL2012 already had the dataset for the rotational fine resolved de-excitation of O_2 by He (36 fine levels; T=5-350K) (Lique 2010), which was calculated using the PES of Groenenboom & Struniewicz (2000). BASECOL20023 was updated with two datasets from Kalugina et al. (2012) concerning the rotational de-excitation of O_2 by o/p-H_2 (7 rotational levels; T=5-150K).

7.16. PN

The PN data (Table B3) include collisions with He and p-H_2 and tackle the rotational process; two recommended datasets are available. BASECOL2012 already had the dataset for the rotational de-excitation of PN by He (31 levels; T=10-300K) (Toboła et al. 2007). BASECOL20023 was updated with a dataset from Najar et al. (2017) concerning the rotational de-excitation of PN by p-H_2 (40 levels; T=10-300K).

7.17. SH

BASECOL2012 already had the dataset for the rotational de-excitation of the fine structure levels of SH by He (Kłos et al. 2009) (60 levels; T=5-350K). On that dataset (Kłos et al. 2009), BASECOL2023 updated the notation for the Kronig parity labels in order for them to agree with VAMDC standards; the scientific content is not changed, but the version of the dataset has changed to v2 and is recommended.

7.18. SiO

The SiO data (Table B3) include collisions with He and H_2, and tackle the rotational and ro-vibrational processes; eight recommended datasets are available.

7.18.1. SiO–He

BASECOL2023 has been updated with two datasets: a low temperature dataset for rotational de-excitation (Dayou & Balança 2006) among 27 rotational levels (T=10-300K) and a more approximate high temperature dataset for ro-vibrational de-excitation (Balança & Dayou 2017) among 246 levels (T=250-10000K).

7.18.2. SiO–H_2

BASECOL2023 was updated with two very rich datasets by Yang et al. (2018b) for collisions with o/p-H_2: the ro-vibrational and rotational de-excitation rate coefficients for SiO ro-vibrational states (v=1, j=1-10) to (v'=0, j'=0-35) in collisions with ortho-H_2 (j=1) and para-H_2(j=0). The rate coefficients for rotational transition of SiO from (v=1, j=1-10) to (v'=1, $j'<j$) and among the first six rotational levels in the ground vibrational state are also included in both the para-H_2 and ortho-H_2 datasets. In addition, the para-H_2 dataset provides the ro-vibrational de-excitation rate coefficients for SiO ro-vibrational states (v=1, j=1-10) to (v'=0, j'=0-34) when para-H_2 is excited from $j(H_2)$=0 to $j(H_2)$=2.

In addition, BASECOL2023 was updated with four datasets (Balança et al. 2018) for the rotational de-excitation of SiO with o/p-H_2: two low temperature datasets (21 levels; T=5-300K) calculated with the CC method, and two high temperature datasets (30 levels; T=5-1000K) obtained with the more approximate CS method (the sets are identified, respectively, as CC and CS in Table B3). The above CC and CS SiO–H_2 datasets are recommended as they could be used to test the influence of different datasets on the radiative transfer results. The user should prefer the CC results over the CS or the infinite order sudden (IOS) approximation results in the relevant temperature range and contact the authors if any doubt. However, the older datasets (Dayou & Balança 2006; Turner et al. 1992) have been set to non-recommended.

7.19. SiS

The SiS data (Table B3) include collisions with He and H_2 and tackle the rotational and ro-vibrational processes; four recommended datasets are available. BASECOL2012 already included a dataset (Vincent et al. 2007) for the rotational de-excitation of SiS by He (26 levels; T=10-200K), two datasets (Kłos et al. 2008) for the rotational de-excitation of SiS by o/p-H_2 (41 levels; T=5K-300K), and one dataset (Toboła et al. 2008) for the ro-vibrational de-excitation of SiS by He (505 levels corresponding to vibration up to v=4 and to rotation up to j=100 with T=100-1500K).

7.20. SO

The SO data (Table B3) include collisions with He and H_2 and tackle the rotational fine structure and ro-vibrational fine structure processes. Six recommended datasets are available.

7.20.1. SO–He

BASECOL2012 already included two datasets for the rotational fine structure de-excitation of SO by He: one dataset (Lique et al. 2005) for 31 fine levels (T=5-50K) and another one (Lique et al. 2006a) for 91 fine levels (T=60-300K). It also included a dataset (Lique et al. 2006c) for the ro-vibrational fine structure de-excitation of SO by He (236 levels; T=300-800K).

7.20.2. SO–H_2

Recently, new extensive calculations have been performed for the ro-vibrational fine resolved de-excitation of SO by o/p-H_2 (Price et al. 2021), where a new 6D PES by Yang et al. (2020) was used. BASECOL2023 has been updated with the corresponding two datasets (Price et al. 2021) that span 273 ro-vibrational transitions up to v=2 for temperatures between 10K and 3000K. BASECOL2012 already included the smaller dataset of Lique et al. (2007) for the rotational fine structure de-excitation of SO by p-H_2 (31 levels; T=5-50K), which already superseded an older dataset from Green (1994) as the 1994 calculations used a CS-H_2 PES.

8. Triatomic molecules with heavy partners

BASECOL2023 contains 31 triatomic species (Table B4) aside from the para-ortho symmetries.

8.1. AlCN, AlNC

One recommended set is available for AlCN and two for AlNC. BASECOL2023 was updated with two datasets (Hernández Vera et al. 2013) concerning the de-excitation by He among the 30 rotational levels of AlCN and of AlNC in the 5K to 100K temperature range. A dataset for the rotational de-excitation of AlNC by p-H_2 (Urzúa-Leiva & Denis-Alpizar 2020) where H_2 is treated as a spherical atom was also added (27 levels; T=5-105K).

8.2. C_3

Four recommended datasets are available for the C_3 molecule. BASECOL2012 included the dataset (Ben Abdallah et al. 2008) for the de-excitation among six rotational levels of C_3 by impact with He (T=5-15K). BASECOL2023 was enriched with three additional datasets: a dataset (Stoecklin et al. 2015) for the ro-vibrational excitation of C_3 by He (23 levels; T=10-155K) and two datasets (Santander et al. 2022) for the rotational de-excitation of C_3 by o/p-H_2 (11 levels; T=5-50K).

8.3. C_2H, C_2D, ^{13}CCH, $C^{13}CH$

Five recommended datasets are available for the $C_2H(X^2\Sigma^+)$ molecule: four datasets for $C_2D(X^2\Sigma^+)$, one for $^{13}CCH(X^2\Sigma^+)$, and one for $C^{13}CH(X^2\Sigma^+)$.

8.3.1. C_2H–He

BASECOL2023 has been upgraded with a new version of the dataset (Spielfiedel et al. 2013) (version 2, 46 levels; T=5-100K) for the de-excitation of the hyperfine levels of C_2H by He, this dataset replaces the previous dataset (Spielfiedel et al. 2012) (version 1, 34 levels; T=5-100K) which had flaws in the calculations and is not recommended.

8.3.2. C_2H–H_2

This system has been updated with a series of datasets of increasing reliability. BASECOL2023 had been updated with a dataset (Dumouchel et al. 2017) for the de-excitation of the first 17 fine levels of C_2H by p-H_2, and the corresponding dataset (Dumouchel et al. 2017) for the de-excitation of the first 34 hyperfine levels of C_2H by p-H_2 (T=2-80K). These datasets were obtained with a 2D PES (Najar et al. 2014) where H_2 is taken as spherical, and where the PES is averaged over H_2 orientations. Those datasets are now labelled as non-recommended as the PES is crude compared to the calculations of Pirlot Jankowiak et al. (2023b).

BASECOL2023 had also been updated with two datasets (Dagdigian 2018a) for the de-excitation from the first 30 hyperfine levels of C_2H by o/p-H_2 (T=10-300K); they were obtained with a newly calculated 4D PES (Dagdigian 2018b). Pirlot Jankowiak et al. (2023b) found an error in those calculations and re-did the dynamical calculations with the same 4D PES (Dagdigian 2018b). BASECOL keeps a trace of the data, and therefore the datasets of Dagdigian (2018a) are kept, but they are labelled as non-recommended. Keeping those datasets of Dagdigian (2018b) is very important, as they were publicly available on both the BASECOL and the LAMDA databases for a certain period of time.

BASECOL2023 was updated with the two recent datasets (Pirlot Jankowiak et al. 2023b) for the de-excitation of 41 fine rotational levels of C_2H by o/p-H_2 (T=5-500K) and the two corresponding datasets (Pirlot Jankowiak et al. 2023b) for the de-excitation of the first 38 hyperfine levels of C_2H by o/p-H_2 (T=5-100K). Those datasets were obtained with the 4D PES of Dagdigian (2018b). The dynamical calculations with p-H_2 include the first two rotational levels of p-H_2, but the state-to-state rate coefficients concern the j(p-H_2) 0-0 transition only.

8.3.3. C_2D–p-H_2

BASECOL2023 had been updated with two datasets (Dumouchel et al. 2017) for the de-excitation from the first 49 hyperfine levels and the first 17 fine levels of C_2D by p-H_2 have been added (T=2-80K); these datasets were obtained with the 2D PES of Najar et al. (2014) averaged over H_2 orientations and shifted to take into account the *D* isotope. Those datasets have been superseded by the datasets of Pirlot Jankowiak et al. (2023b), and they are labelled as non-recommended.

BASECOL2023 had been updated with two datasets (Pirlot Jankowiak et al. 2023b) for the state-to-state de-excitation from the 31 fine structure levels of C_2D with o/p-H_2 (T=5-200K), and the corresponding two datasets (Pirlot Jankowiak et al. 2023b) for the state-to-state de-excitation from the first 55 hyperfine levels of C_2D by o/p-H_2 (T=5-100K). The dynamical calculations with p-H_2 include the first two rotational levels of p-H_2, but the state-to-state rate coefficients concern the j(p-H_2) 0-0 transition only.

8.3.4. ^{13}CCH, $C^{13}CH$ with p-H_2

BASECOL2023 has been updated with two datasets (Pirlot Jankowiak et al. 2023a) for the hyperfine and fine resolved rotational de-excitation of $C^{13}CH$ and ^{13}CCH by p-H_2. Both datasets involve transitions among 98 hyperfine levels for temperatures between 5K and 100K. The hyperfine couplings include a first coupling with the ^{13}C nuclear spin leading to the F_1 quantum number and then a coupling to the hydrogen nuclear spin leading to the F quantum number.

8.4. C_2H^-

Two recommended datasets are available for the C_2H^- molecule. BASECOL2023 was updated with two datasets for the rotational de-excitation of C_2H^- by He; one dataset (Gianturco et al. 2019) involves nine rotational levels (T=5-100K), and the other dataset (Dumouchel et al. 2012) involves 13 rotational levels (T=5-100K). Both datasets were calculated with the same PES (Dumouchel et al. 2012); the cross-sections were obtained over the same range of energies up to 1000 cm^{-1} with the close coupling method; therefore, the rate coefficients should be equivalent, as shown in Figure C.3.

8.5. C_2N^-

One recommended dataset is available for the open shell C_2N^- ($X^3\Sigma^-$) molecule. BASECOL2023 was updated with a dataset (Franz et al. 2020) for the de-excitation among rotational levels of C_2N^- in collision with He (16 levels; T=5-100K). In that calculation, the electronic structure of C_2N^- has been ignored, and the energy levels are labelled with the spin free quantum number N; they also calculated a new PES for the C_2N^--He system.

8.6. C_2O

One recommended dataset is available for the open shell $C_2O(X^3\Sigma^-)$ molecule. BASECOL2023 was upgraded with a dataset (Khadri et al. 2022b) concerning the de-excitation of C_2O in collision with He (31 levels; T=2-80K); this dataset was obtained with a newly developed PES (Khadri et al. 2022b). This is part of a series of calculations that explore the excitation of long carbon chains (see below).

8.7. CH_2

Four recommended datasets are available for the asymmetric open shell CH_2 (X^3B_1) molecule.

BASECOL2023 was upgraded with four new datasets (Dagdigian 2021b) for the CH_2 molecule in its para and ortho symmetries: datasets for the de-excitation from the first 69 hyperfine levels of o-CH_2 by o/p-H_2 and from the first 27 rotational levels of p-CH_2 by o/p-H_2 were added for temperatures between 5K and 300K. Those four datasets were obtained with a newly calculated PES (Dagdigian 2021c), and the splittings due to the electron spin were treated using a recoupling method. For o-CH_2 the splittings due to the nuclear spin were treated with the M_J randomisation approximation (Alexander & Dagdigian 1985).

8.8. CO_2

One recommended dataset is available for the CO_2 molecule. BASECOL2023 was upgraded with a collisional dataset (Godard Palluet et al. 2022) for the rotational de-excitation of CO_2 by He (21 levels; T=4-300K); this dataset was calculated with a newly developed PES (Godard Palluet et al. 2022).

8.9. HCN

Six recommended datasets are available for the HCN molecule.

8.9.1. HCN–He

BASECOL2012 already contained the dataset for the excitation of the 26 rotational levels of HCN by He (Dumouchel et al. 2010; Sarrasin et al. 2010). This dataset uses the sophisticated PES of Toczyłowski et al. (2001) and therefore supersedes the calculations by Green & Thaddeus (1974). When hyperfine resolved lines are observed, the dataset of Monteiro & Stutzki (1986) could be used in the absence of other data, though it is not reliable because of the poor PES used in the dynamical calculations. This dataset is currently indicated as non-recommended, and additional calculations of hyperfine rate coefficients should be performed. As an alternative, the rotational rate coefficients of Dumouchel et al. (2010); Sarrasin et al. (2010) could be used to produce hyperfine levels transitions using an IOS approach (Corey & McCourt 1983).

8.9.2. HCN–H_2

The excitation of HCN by para and ortho-H_2 has led to the two datasets (Hernández Vera et al. 2017) of BASECOL2023, that include the excitation of 26 rotational levels of HCN up to 500K, with calculations based on the PES of Denis-Alpizar et al. (2013). Part of this work is an extension of the work of Hernández Vera et al. (2014), where the excitation of 13 levels by para H_2 below 100K was calculated, and the data are identical in the overlapping region. The latter dataset (Hernández Vera et al. 2014) is kept in BASECOL2023, as one objective of BASECOL is to curate data published in journals.

Using those highly accurate rate coefficients and an IOS recoupling method, Goicoechea et al. (2022) calculated the hyperfine resolved rate coefficients for HCN in collision with o/p-H_2, the two corresponding datasets (34 levels; T=5-500K) (Goicoechea et al. 2022) are in BASECOL2023. Those datasets supersede the hyperfine HCN-p-H_2 dataset by Ben Abdallah et al. (2012) calculated with a simpler PES averaged over three orientations of H_2. It was mentioned in Hernández Vera et al. (2014) that the HCN-p-H_2 calculations of Ben Abdallah et al. (2012) led to significant inaccuracies, in particular at low temperatures. Therefore, the dataset of Ben Abdallah et al. (2012) is labelled as non-recommended.

Finally, for cometary applications, BASECOL2023 was updated with a dataset (Dubernet & Quintas-Sánchez 2019) with thermalised rate coefficients for the de-excitation of HCN (8 levels; T=5-150K) by p-H_2O. The calculations use a new 5D PES (Quintas-Sánchez & Dubernet 2017) and the CS method, where the basis sets are not fully converged (about 20%). The thermalised rate coefficients are obtained from the state-to-state rate coefficients summing over the final states of para-H_2O and averaging over the initial rotational states of para-H_2O.

8.10. HNC

Five recommended datasets are available for the HNC molecule for collisions with He and o/p-H_2. BASECOL2012 already included the dataset (Dumouchel et al. 2010; Sarrasin et al. 2010) for the excitation among the 26 rotational levels of HNC by He calculated with the new PES of Sarrasin et al. (2010) (T=5-500K), and two datasets (Dumouchel et al. 2010) for the rotational de-excitation among eleven rotational levels of HNC by o/p-H_2 (T=5-100K). The p-H_2 dataset included the excitation between the ground level and the first excited state of p-H_2, as well as de-excitation of HCN rotational levels for j=2 of p-H_2. The o-H_2 dataset was calculated with an extended basis for $H_2(j=1,3)$.

BASECOL2023 has been updated with two datasets (Hernández Vera et al. 2017) for the de-excitation of HNC by p-$H_2(j=0)$ and o-$H_2(j=1)$ (26 levels; T=5-500K). The p-H_2 dataset was calculated with an extended basis set for p-$H_2(j=0,2)$, but the o-H_2 dataset was calculated with o-H_2 (j=1) only. The new datasets (Hernández Vera et al. 2017) are identical or similar for the 11 lowest transitions and for temperatures below 100K to the previous datasets of Dumouchel et al. (2010) when H_2 stays, respectively, in its lowest level, j=0 or j=1. The datasets of Dumouchel et al. (2010) are recommended as the quality of the data is identical to those of Hernández Vera et al. (2017) for collision with both p-H_2 and o-H_2; in addition, the dataset of Dumouchel et al. (2010) provides information on the behaviour of rate coefficients with $j(H_2)$=2.

8.11. HCO^+, DCO^+, $HC^{17}O^+$

Three recommended datasets are available for HCO^+: one for DCO^+ and one for $HC^{17}O^+$. BASECOL2023 was upgraded with a dataset (Tonolo et al. 2021) for the de-excitation of six rotational levels of HCO^+ in collision with He (T=5K-100K) calculated with their new PES (Tonolo et al. 2021) and with two datasets (Denis-Alpizar et al. 2020) for the rotational de-

excitation of HCO^+ by o/p-H_2 (22 levels; T=10K-200K), calculated with their new 4D PES (Denis-Alpizar et al. 2020). The previous dataset for the de-excitation of HCO^+ by p-H_2 (j=0) from Flower (1999b), which used an old PES (Monteiro 1985), is now outdated because of the quality of the PES, and it is indicated as non-recommended.

A new dataset (Denis-Alpizar et al. 2020) was added for the rotational de-excitation of DCO^+ in collision with p-H_2 (22 levels; T=10K-200K) calculated with the same 4D PES (Denis-Alpizar et al. 2020) as HCO^+–H_2. BASECOL2012 included a low-quality dataset (Pagani et al. 2012) for the hyperfine structure resolved de-excitation of DCO^+ by p-H_2 obtained with an IOS recoupling technique using the HCO^+–p-H_2 rotational rate coefficients of Flower (1999b), the latter being now superseded. Nevertheless, the dataset of Pagani et al. (2012) is left as recommended as it is the only available dataset. However, we would recommend using the newly calculated rotational dataset of DCO^+–p-H_2 (Denis-Alpizar et al. 2020) to calculate new hyperfine rate coefficients for this system. Finally, we have added a dataset (Tonolo et al. 2022) for the de-excitation among the 33 first hyperfine levels of $HC^{17}O^+$ with p-H_2; in these calculations, the H_2 projectile has been treated as a spherical body and an average of the potential based on five orientations of H_2 has been employed for the scattering calculations.

8.12. HCO

Two recommended datasets are available for the HCO asymmetric open shell molecule. BASECOL2023 was upgraded with two datasets (Dagdigian 2020b) for the de-excitation among hyperfine resolved rotational levels of HCO by o/p-H_2 (86 levels; T=5-200K). Those rate coefficients were obtained with a new PES (Dagdigian 2020d), the splittings due to the electron spin was treated using a recoupling method, while the splittings due to the nuclear spin was treated with the M_J randomisation approximation (Alexander & Dagdigian 1985).

8.13. HCP

Two recommended datasets are available for the HCP molecule. BASECOL2012 already had a dataset (Hammami et al. 2008b) for the rotational de-excitation of HCP by He (16 levels; T=20-200K) and a dataset (Hammami et al. 2008) for the rotational de-excitation of HCP by p-H_2 (11 levels; T=10-70K). In both systems, a new PES was calculated; for the HCP–p-H_2 system, the H_2 projectile was treated as a spherical body and an average of the potential based on five orientations of H_2 was employed for the scattering calculations.

8.14. HCS^+

Two recommended datasets are available for the HCS^+ molecule. BASECOL2023 was updated with a dataset (Dubernet et al. 2015) for the rotational de-excitation of HCS^+ by He (20 levels; T=5-100K) calculated with a new PES (Dubernet et al. 2015). This dataset supersedes the dataset of Monteiro (1984) because of better quality of the PES and of the dynamical calculations, the dataset of Monteiro (1984) is indicated as non-recommended.

A new dataset (Denis-Alpizar et al. 2022) for the rotational de-excitation of HCS^+ by p-H_2 has been added; this dataset has been obtained with a new PES (Quintas-Sánchez et al. 2021). The authors mention that this dataset can be used for collisions with o-H_2 to a good approximation.

8.15. H_2O

Twenty-two recommended datasets are currently available for the H_2O molecule.

8.15.1. H_2O–He

BASECOL2023 was updated with two datasets (Yang et al. 2013) for the de-excitation of rotational levels of o/p-H_2O by He (10 levels; T=2-3000K); these calculations have used the PES from Patkowski et al. (2002). BASECOL2012 already had the two datasets from Green et al. (1993) (45 levels; T=20-2000K) that had been calculated with the PES of Maluendes et al. (1992). Those datasets are still marked as recommended as they span more transitions, and the agreement between both sets are reasonably good, see Figure C.4. However, at low temperatures, the data of Yang et al. (2013) show significant differences with the previous rates.

8.15.2. H_2O with o/p-H_2 and thermalised H_2

There are three types of calculation for the rotational de-excitation of H_2O with H_2: highly accurate quantum calculations (mostly CC calculations) (Daniel et al. 2011, 2010; Dubernet et al. 2009), quasi-classical calculations (QCT) (Faure et al. 2007a), and more approximate quantum CS calculations (Żółtowski et al. 2021) that provide rate coefficients among twice the number of rotational levels than the two other sets of calculations.

BASECOL2012 contained the four state-to-state rate coefficients datasets (Daniel et al. 2011, 2010; Dubernet et al. 2009) for the rotational de-excitation of o/p-H_2O by o/p-H_2(j) (45 levels; T=5-1500K) where the transitions among H_2 levels have been considered up to $j(H_2)$= 4 for some water transitions; those datasets have been obtained with a 5D average of the 9D PES of Valiron et al. (2008) and quantum calculations (mostly close coupling) for the dynamics of the nuclei. Daniel et al. (2011) completed calculations of respectively Dubernet et al. (2009) and Daniel et al. (2010). A package is distributed in the 'tools' section of the BASECOL website in order to calculate effective and thermalised rate coefficients. Those results superseded the four datasets of Phillips et al. (1996) (5 levels; T=20-140K) calculated with the PES of Phillips et al. (1994), which are now marked as non-recommended.

BASECOL2012 contained four datasets (Faure et al. 2007a) calculated with a 5D average of the 9D PES of Valiron et al. (2008) and with quasi-classical trajectories (45 levels; T=20-2000K). Though those data have been obtained with a less precise method than the results of Daniel et al. (2011, 2010); Dubernet et al. (2009), and though they might show differences of as much as a factor of three, they are still marked as recommended as an alternative choice for users.

BASECOL2023 was updated with two datasets (Żółtowski et al. 2021) for the rotational de-excitation of o/p-H_2O by p-H_2 (97 levels; T=10-2000K). The authors used the 5D average of the 9D PES of Valiron et al. (2008), but this potential was further approximated using the adiabatic hinder rotor approximation proposed by Scribano et al. (2012), reducing its dimensionality to 3D, where the H_2 molecule is treated as a pseudo-atom. The authors indicate that the precision of the rate coefficients can

be between a factor of two and three compared to quantum close coupling calculations using a full 5D PES. The datasets are nevertheless marked recommended, as they provide a very large extension in the number of transitions. BASECOL2012 contained two datasets (Faure et al. 2007a) calculated with the 9D PES of Valiron et al. (2008) for the ro-vibrational de-excitation of o/p-H_2O with fully thermalised H_2 (411 levels; T=200-5000K).

8.15.3. H_2O–H

BASECOL2023 was updated with two datasets (Daniel et al. 2015) for the rotational de-excitation of o/p-H_2O by H (45 levels; T=5-1500K). These datasets were obtained with the PES of Dagdigian & Alexander (2013).

8.15.4. H_2O–H_2O

BASECOL2023 has been updated with four datasets for the rotational de-excitation of o/p-H_2O by thermalised H_2O; those datasets are intended for cometary and planetary atmospheres applications. Two datasets (Boursier et al. 2020) for transitions among 59 o/p-H_2O levels (T=100-800K) have been obtained with a crude PES and with semi-classical calculations; two other datasets (Mandal & Babikov 2023a) for transitions among 21/22 o/p-H_2O levels (T=5K-1000K) were obtained with the MQCT method (Mandal & Babikov 2023b; Mandal et al. 2022), a truncated expansion of the PES of Jankowski & Szalewicz (2005) and extrapolations of cross-sections at low and high collision energy. All of these datasets were obtained using approximate scattering methods that involve the symmetrisation of cross-sections computed for excitation and quenching to ensure that the final data satisfy the principle of detailed balance, as explained in detail in the references cited (Boursier et al. 2020; Mandal & Babikov 2023a).

8.16. D_2O, HDO

Two recommended datasets are currently available for the D_2O molecule, and three are available for the HDO molecule. BASECOL2023 was updated with two datasets (Faure et al. 2012) for the rotational de-excitation of o/p-D_2O by p-H_2 (6 levels; T=5-100K); these datasets were obtained with the PES of Valiron et al. (2008) and with quantum calculations for the dynamics of the nuclei.

BASECOL2012 already included a dataset (Green 1989) for the rotational de-excitation of HDO by He (34 levels; T=50-500K). BASECOL2023 has been updated with two datasets (Faure et al. 2012); one dataset provides thermalised rotational de-excitation rate coefficients of HDO by p-H_2 (30 levels; T=5-300K) and the other includes rotational de-excitation rate coefficients of HDO by o-H_2 (j=1). These datasets were obtained with the PES of Valiron et al. (2008) and with quantum calculations for the dynamics of the nuclei.

8.17. H_2S

Four recommended datasets are available for the closed-shell asymmetric H_2S molecule. BASECOL2023 was updated with four datasets (Dagdigian 2020a) for the rotational de-excitation of o/p-H_2S by o/p-H_2 (19 levels; T=5-500K). These datasets were calculated with a new 4D PES (Dagdigian 2020c).

8.18. MgCN, MgNC

Two recommended datasets are available for MgCN, and there are two for MgNC. BASECOL2023 was updated with two datasets (Hernández Vera et al. 2013) concerning the rotational de-excitation by He among the 36 rotational levels of MgCN and of MgNC (T=5-100K) and with two datasets (Hernández Vera et al. 2013) for the de-excitation among the fine resolved structures of MgCN and MgNC (T=5-100K). The de-excitation among fine levels uses a recoupling technique based on the IOS approximation (Corey & McCourt 1983).

8.19. NH_2

Four recommended datasets are available for the asymmetric open shell NH_2 (X^3B_1) molecule.

The NH_2 (X^3B_1) molecule presents a fine and hyperfine structure, but presently no collisional studies including either the electronic or the nuclear spins have been performed. BASECOL2023 was updated with four datasets (Bouhafs et al. 2017a) for the de-excitation among 15 spin free rotational levels of p-NH_2 and o-NH_2 by o-/p-H_2 (T=10-150K); these datasets were obtained with a 4D PES (Bouhafs et al. 2017a) constructed from the 9D global PES of the ground electronic state of NH_4 (Li & Guo 2014).

8.20. N_2H^+

Four recommended datasets are available for the N_2H^+ molecule. BASECOL2012 already included two datasets (Daniel et al. 2005) calculated with a new PES (Daniel et al. 2004) for the de-excitation among seven rotational and among 55 hyperfine levels of N_2H^+ by He. The dataset of Green (1975) was superseded and is labelled as non-recommended.

BASECOL2023 was updated with a dataset (Balança et al. 2020) for the de-excitation among 26 rotational levels of N_2H^+ by p-H_2 (T=5-500K). The data were obtained with the adiabatic hindered rotor (AHR) approach (Li et al. 2010; Zeng et al. 2011), which reduced the 4D PES of Spielfiedel et al. (2015) to a 2D PES, and thus did not take into account the structure of the H_2 projectile. In addition, BASECOL2023 was updated with a dataset (Lique et al. 2015) for the de-excitation among 64 hyperfine levels of N_2H^+ by p-H_2. This dataset was obtained with the same AHR approach, the same PES (Spielfiedel et al. 2015), and with a recoupling technique (Daniel et al. 2004).

8.21. OCS

Three recommended datasets are available for the OCS molecule. New work is certainly needed for this molecule. BASECOL2012 already included a dataset (Green & Chapman 1978) for the rotational de-excitation of OCS by p-H_2 (13 levels; T=10-100K), and a dataset (Flower 2001b) for the rotational de-excitation of OCS by He (27 levels; T=10-150K). The dataset with p-H_2 was obtained with a very crude PES and the CS method. BASECOL2023 was updated with a dataset (Chefai et al. 2018) for the de-excitation of OCS by Ar, for which a new PES was calculated (Chefai et al. 2018).

8.22. o-SiC_2

One recommended dataset is available for the o-SiC_2 molecule. BASECOL2012 already included a dataset (Chandra & Kegel 2000) for the rotational de-excitation of o-SiC_2 by He (40 levels;

T=25-125K). The authors used an infinite order sudden approximation method, extended the work of Palma & Green (1987), and claimed that their results applied to the H_2 projectile. We redid the calculations, and it is clear that their results correspond to a collision with He.

8.23. SO_2

Three recommended datasets are available for the SO_2 molecule. BASECOL2012 already included a dataset (Green 1995) for the rotational de-excitation of SO_2 by He (50 levels; T=25-125K) with the PES of Palma (1987) and an IOS method. BASECOL2012 included two datasets (Cernicharo et al. 2011) for the de-excitation of SO_2 by o/p-H_2 (31 levels; T=5-30K). These datasets were obtained with a 5D PES from Spielfiedel et al. (2009) and with the close coupling method.

9. Molecules with more than three atoms with heavy partners

The general table (Table B5) presents collisional datasets for 26 molecules with more than three atoms.

9.1. C_3H_2

Two recommended datasets are available for the C_3H_2 molecule. BASECOL2012 already included a dataset (Chandra & Kegel 2000) for the rotational de-excitation of o/p-C_3H_2 by He (47/48 levels; T=30-120K). The authors used the IOS method, extended the work of Green et al. (1987), and claimed that their excitation rate coefficients applied to the H_2 projectile. We re-did the calculations and it is clear that their results correspond to a collision with He. The current datasets provide the de-excitation rate coefficients obtained by detailed balance using the JPL database (Pearson et al. 2010) spectroscopic data. It should be noted that more precise datasets were calculated by Avery & Green (1989), but for fewer levels. They provided CS rate coefficients among the 16 lowest ortho levels and the 17 lowest para levels for three temperatures (T = 10, 20, 30 K); they used the same PES (Green et al. 1987). The latter calculation is not in BASECOL.

9.2. C_3O, C_3S

One recommended dataset is available for C_3O and one for C_3S. BASECOL2023 was updated with a dataset (Bop et al. 2022b) for the rotational de-excitation of C_3O by He (31 levels; T=5-150K) calculated with the PES of Khadri & Hammami (2019), and a dataset (Sahnoun et al. 2020) for the rotational de-excitation of C_3S by He (11 levels; T=2-25K); in the latter calculation the authors calculated a new PES.

9.3. C_4

One recommended dataset is available for the C_4 ($X^3\Sigma_g^-$) molecule. BASECOL2012 already included a dataset (Lique et al. 2010a) for the fine structure resolved rotational de-excitation of C_4 by He (30 levels; T=5-50K). The authors calculated a new PES.

9.4. C_4H^-

Two recommended datasets are available for the C_4H^- molecular ion. BASECOL2023 was updated with two datasets (Balança et al. 2021) for the rotational de-excitation of C_4H^- by o/p-H_2 (30 levels; T=5-100K). A new PES was calculated by the authors.

9.5. C_5,C_5O, C_5S

One recommended dataset is available for C_5, one is available for C_5O, and one is available for C_5S. BASECOL2023 was updated with a dataset (Chefai et al. 2021) for the rotational de-excitation of C_5 by He (15 levels; T=5-300K) and a dataset (Khadri et al. 2020) for the rotational de-excitation of C_5S by He (51 levels; T=2-100K). In both cases the respective authors calculated a new PES. In addition, it has been updated with a dataset (Bop et al. 2022b) for the rotational de-excitation of C_5O by He (31 levels; T=5-150K). These calculations were performed with the PES of Khadri et al. (2022a).

9.6. C_5H^+

One recommended dataset is available for the C_5H^+ molecular ion. BASECOL2023 has been updated with a dataset (Khadri et al. 2023) for the rotational de-excitation of C_5H^+ by He (16 levels; T=5-100K). The authors calculated a new 2D PES. This calculation follows the recent discovery of this new molecule in TMC-1 (Cernicharo et al. 2022).

9.7. C_6H^-, C_6H

Two recommended datasets are available for C_6H ($^2\Pi$) and three for C_6H^-. BASECOL2023 was updated with two datasets (Walker et al. 2018): one for the fine resolved rotational de-excitation of C_6H by He (122 levels; T=5-100K) and one for the hyperfine resolved de-excitation for the same system (52 levels; T=5-100K). The authors calculated a new PES.

Three new datasets (Walker et al. 2017) for the excitation of the close-shell anion C_6H^- were added: one dataset for the rotational de-excitation of C_6H^- by He (11 levels; T=5-100K) and two datasets for the rotational de-excitation of C_6H^- by o/p-H_2 (31 levels; T=5-100K). The three datasets were obtained with a new PES (Walker et al. 2016).

9.8. CH_3CN, CH_3NC

Two recommended datasets are available for CH_3CN and two are available for CH_3NC. BASECOL2023 was updated with four datasets (Ben Khalifa et al. 2023) for the rotational de-excitation of o/p-CH_3CN (52/75 levels; T=7-100K) and of o/p-CH_3NC (66/63 levels; T=7-100K) by He. These collisional datasets were calculated with the PES of Ben Khalifa et al. (2022).

9.9. CH_3OH

Fourteen recommended datasets are available for CH_3OH; they handle rotational processes for three torsional states and for ro-torsional processes. The datasets existed in BASECOL2012, but they were very recently imported to BASECOL2023 as we needed to take decisions about the labelling of the energy levels.

The current BASECOL labelling of levels is J, K ($=K_a$), v_t the torsional quantum number, and the ro-torsional symmetry of

the wave function (A or E). In addition, for A states the pseudo-parity is indicated by a + or − symbol; this pseudo-parity comes from the two possible linear combinations of basis set functions as explained in Herbst et al. (1984) and Hougen et al. (1994). Therefore, the VAMDC rovibSym label is used as a ro-torsional symmetry label and follows the convention $A+$, $A-$, $E1$ (equivalent to "E with positive K-sign") and $E2$ (equivalent to "E with negative K-sign") with the symmetric quantum numbers J and K (>0). CH_3OH is currently identified by the stcs VAMDC case (see Table A1), as no other case can fit this description.

Those notations are implicitly used in the traditional output of the JPL (Pearson et al. 2010) database, and both in the traditional and the VAMDC access of the HITRAN database (Gordon et al. 2022). It should be noted that the JPL quantum numbers are incomplete. The rovibSym label is omitted, and the pseudo-parity quantum number is included for the A-symmetry states only. By deduction, the levels without pseudo-parity belong to the E-symmetry, and JPL uses the K-signed notation.

It is possible to use the usual labelling of the C_{3v} symmetry group, that is the asymmetric rotational quantum numbers (J, K_a (=K), K_c), the v_t quantum number, and the ro-torsional A or E symmetry. An example of these notations is provided in the CDMS (Müller et al. 2005) database; these notations imply that their VAMDC output uses an asymmetric top closed shell (asymcs) case.

Hougen et al. (1994) explained how to transform notations from one label to the other. In addition, the supplementary material of Xu et al. (2008) identifies the energy levels with notations that allow to find the two ways of labelling. For A-symmetry the states are identified with J, $K_a = K$, K_c, v_t and the pseudo-parity; for the E-symmetry, the states are identified with J, K-signed, and K_c, v_t.

9.9.1. CH_3OH-He

Two datasets (Rabli & Flower 2011) are available for the ro-torsional de-excitation of A-CH_3OH and E-CH_3OH by He (150 levels; T=10-400K). The authors used the PES of Pottage et al. (2002). Six datasets (Rabli & Flower 2010b) are available for the rotational de-excitation of A/E-CH_3OH by He, with A/E-CH_3OH in respectively the ground, the $v_t = 1$ and the $v_t = 2$ torsional states (256 levels; T=10-200K); the authors used the PES of Pottage et al. (2002). It should be noted that those calculations were carried out with a maximum value of j=15, which means that there are missing higher j rotational levels for energy levels lying above 200 cm^{-1}.

9.9.2. CH_3OH-p-H_2

Six datasets (Rabli & Flower 2010a) are available for the rotational de-excitation of A/E-CH_3OH by p-H_2, with A/E-CH_3OH in the ground, the v_t=1, and the $v_t = 2$ torsional states, respectively (256 levels; T=10-200K); the authors used the PES of Pottage et al. (2004). Again, it should be noted that those calculations are carried out with a maximum value of j=15, which means that there are missing higher j rotational levels for energy levels lying above 200 cm^{-1}.

9.10. CNCN

One recommended dataset is available for CNCN. BASECOL2023 was updated with a dataset (Ndaw et al. 2021) for the rotational de-excitation of CNCN by He (30 levels; T=5-150K); the authors calculated a new PES.

9.11. H_2CO

Four recommended datasets are available for the H_2CO molecule. BASECOL2012 already included two datasets (Green 1991) for the rotational de-excitation of o/p-H_2CO by He (40/41 levels; T=10-300K) that used the PES of Garrison & Lester (1975) and two datasets (Troscompt et al. 2009) for the rotational de-excitation of o-H_2CO by o/p-H_2 (10 levels; T=5-100K), where the authors calculated a new PES.

9.12. H_3O^+

Four recommended datasets are available for the H_3O^+ molecular ion. BASECOL2023 has been updated with four datasets (Demes et al. 2022) for the rotational de-excitation of the lowest 11 rotation-inversion levels of o-H_3O^+ with o/p-H_2 and of the 21 lowest rotation-inversion levels of p-H_3O^+ with o/p-H_2, for temperatures between 10K and 300K. The collisional datasets with p-H_2 include calculations described in Demes et al. (2022) and in Demes et al. (2021), and all four datasets were calculated with the PES of Demes et al. (2020).

9.13. HC_3N

Seven recommended datasets are available for the HC_3N molecule. BASECOL2012 already included a dataset (Wernli et al. 2007a) for the rotational de-excitation of HC_3N by He (11 levels; T=10-40K). This dataset is considered to supersede the dataset of Green & Chapman (1978) (21 levels; T=10-80k), as the authors (Green & Chapman 1978) used a Gordon-Kim PES (Gordon & Kim 1972) and the dynamics of the collision is treated with the quasi-classical trajectory approach. Therefore, the dataset of Green & Chapman (1978) is marked as non-recommended.

BASECOL2012 included a dataset (Wernli et al. 2007a) for the rotational de-excitation of HC_3N by p-H_2 (j=0) (51 levels; T=10-100K). This dataset suffered from errors in the calculations, and the authors (Wernli et al. 2007b) indicated that the uncertainties on rate coefficients might be around 20%. This dataset is now indicated as non-recommended, as new calculations are available.

BASECOL2023 was updated with three datasets (Faure et al. 2016) for the rotational de-excitation of HC_3N by p-H_2 and o-H_2 (38 levels; T=10-300K). One dataset presents the state-to-state rate coefficients of HC_3N by p-H_2 in its ground rotational state j=0; a second dataset presents the thermalised rate coefficients of HC_3N by p-H_2; the third dataset corresponds to the state-to-state rate coefficients of HC_3N by o-H_2 (j=1) that can be used as thermalised rate coefficients. The calculations were not performed for j(H_2) larger than 1; thus, assumptions were performed in order to obtain the thermalised rate coefficients (see Faure et al. (2016) for the methodology used for the thermalisation). It should be noted that close coupling calculations were used below j(HC_3N)=30. For HC_3N levels between j(HC_3N) = 31 and 37, only QCT rate coefficients for para-H_2(j = 0) were available, and this set was employed directly for both para-H_2 and ortho-H_2 (no thermal averaging).

In addition, BASECOL2023 was updated with three datasets (Faure et al. 2016) for the de-excitation among hyperfine resolved rotational levels of HC_3N by p-H_2 and o-H_2

(61 levels; T=10-100K). Those datasets were obtained from the above-mentioned three rotational rate coefficient datasets using the scaled-infinite-order-sudden-limit method (Neufeld & Green 1994; Lanza & Lique 2014), which was checked against recoupling calculations.

9.14. HNCCC, HCCNC

Two recommended datasets are available for the HNCCC molecule, and two are available for HCCNC. BASECOL2023 was updated with two datasets (Bop et al. 2021) for the rotational de-excitation of HNCCC by o/p-H_2 (30 levels; T=5-80K) and with two datasets (Bop et al. 2021) for the rotational de-excitation of HCCNC by o/p-H_2 (30 levels; T=5-80K). The datasets were obtained with a new PES (Bop et al. 2019a).

9.15. HMgNC

One recommended dataset is available for the HMgNC molecule. BASECOL2023 was updated with a dataset (Amor et al. 2021) for the rotational de-excitation of HMgNC by He (14 levels; T=5-200K); the authors calculated a new PES.

9.16. $HOCO^+$

One recommended dataset is available for the $HOCO^+$ molecule. BASECOL2012 already included a dataset (Hammami et al. 2007) for the rotational de-excitation of $HOCO^+$ by He (25 levels; T=10-30K); the dataset was calculated with the PES of Hammami et al. (2004).

9.17. $NCCNH^+$

One recommended dataset is available for the $NCCNH^+$ molecule. BASECOL2023 was updated with a dataset (Bop et al. 2018) for the rotational de-excitation of $NCCNH^+$ by He (11 levels; T=5-100K); the authors calculated a new PES.

9.18. NH_3

Sixteen recommended datasets are available for the NH_3 molecule.

9.18.1. NH_3-He

BASECOL 2012 already included two datasets (Machin & Roueff 2005) for the rotational de-excitation of o/p-$NH_3$by He (22/16 levels; T=5-300K). Those datasets were obtained with the PES of Hodges & Wheatley (2001).

9.18.2. NH_3-H_2

The first calculations for the excitation of o/p-NH_3 by para-H_2 were performed by Danby et al. (1986, 1987) in the temperature range from 15K to 300K, subsequently improved and extended to 17 levels for ortho-NH_3 and to 24 levels for para-NH_3 by Danby et al. (1988). Therefore, the datasets of Danby et al. (1986, 1987) are marked as non-recommended.

The next set of calculations for the excitation of o/p-NH_3 by p-H_2 were performed by Maret et al. (2009) using their newly calculated PES for ten levels of p-NH_3 and six levels of ortho-NH_3 in the temperature range from 5K to 100K; those datasets were already in BASECOL2012.

BASECOL2023 was updated with four datasets (Bouhafs et al. 2017b) for the rotational de-excitation of o/p-NH_3 by o/p-H_2. The work of Bouhafs et al. (2017b) used the same PES (Maret et al. 2009), extended the number of transitions to 17 o-NH_3 and 34 p-NH_3 levels, and increased the temperature range up to 200K. The calculations of Bouhafs et al. (2017b) are of better quality than those of Danby et al. (1988), as their basis set included the $j(H_2)$=2 level for collision with p-H_2. However, the calculations of Bouhafs et al. (2017b) did not include the temperature T=5K.

Very recently and using the same PES (Maret et al. 2009), close coupling calculations were performed up to 500K by Demes et al. (2023), where most of the rotation-inversion levels of ammonia were considered below the first vibrational excitation threshold, leading to a total of 33 ortho- and 62 para-NH_3 states. Those calculations were carried out with a basis set that includes $j(H_2)$=0, 2 for p-H_2 and $j(H_2)$= 1 for o-H_2.

Therefore, BASECOL2023 was updated with four datasets (Demes et al. 2023) for the state-to-state rotational de-excitation of o(33 levels)/p(62 levels)-NH_3 by o/p-H_2 between 100K and 500K. It should be noted that the two datasets for o/p-NH_3 with p-H_2 include the state-to-state rate coefficients involving all transitions between j(p-H_2)=0 and j(p-H_2)=2 (i.e. 0-0, 0-2, 2-0 and 2–2 transitions). In addition, two datasets (Demes et al. 2023) for thermalised rate coefficients of o(33 levels)/p(62 levels)-NH_3 with p-t-H_2, built upon the previously mentioned state-to-state rate coefficients ($j(H_2)$=0,2), are included.

As a conclusion, we choose to remove the recommendation of the results of Danby et al. (1988), and we kept the datasets of Maret et al. (2009), of Bouhafs et al. (2017b), and of Demes et al. (2023), as recommended. These should overlap and agree in some regions of temperature and transitions. We did this so that the user can access all those data through VAMDC.

9.18.3. NH_3-H

BASECOL2023 was updated with two datasets (Bouhafs et al. 2017b) for the de-excitation of 34 levels of p-NH_3 by H and for the de-excitation of 17 levels of o-NH_3 by H. They are calculated with the PES of Li & Guo (2014).

9.19. NH_3 isopotologues

Four recommended datasets are available for the NH_2D, four are available for ND_2H, and three are available for ND_3. BASECOL2012 already included two datasets (Machin & Roueff 2006) for the rotational de-excitation of o/p-NH_2D by He (9 levels; T=5-100K) and two datasets (Machin & Roueff 2007) for the rotational de-excitation of o/p-ND_2H by He (9 levels; T=5-100K). The four datasets were calculated with a modified version of the PES of Hodges & Wheatley (2001) to account for isotopic shift.

BASECOL2023 was updated with two datasets (Daniel et al. 2014) for the rotational de-excitation of o/p-NH_2D by p-H_2 (79 levels; T=5-300K), two datasets (Daniel et al. 2016) for the rotational de-excitation of o/p-ND_2H by p-H_2 (16 levels; T=5-50K), and three datasets (Daniel et al. 2016) for the rotational de-excitation of o/p/meta-ND_3 by p-H_2 (16/9/9 levels; T=5-50K). The seven new datasets were calculated with a modified version of the PES of Maret et al. (2009) to account for isotopic shift. It should be noted that the collisional treatment ignored the para or meta specificity of ND_3, so the theoretical results for the para

and meta spin isomers are identical. However, specific calculations were performed for the ortho-ND_3 spin isomer.

10. Other information displayed on the BASECOL website

Two other sections are displayed on the BASECOL website: the contacts section, which provides the information about the maintainers of the BASECOL, and the tools section, where tools sent by producers and by other teams are provided. Currently, there is a package called the water rate package, which makes it possible to use the fitting functions of the H_2O-H_2 rate coefficients (Daniel et al. 2011, 2010; Dubernet et al. 2009) in order to obtain state to state, effective and thermalised rate coefficients; the package contains an option to create outputs in the RADEX format [15].

A link to the VAMDC SPECTCOL tool is also provided; the aim of the client tool SPECTCOL [16] is to associate spectroscopic data extracted from spectroscopic databases through VAMDC, with collisional data provided by collisional databases. It can also be used to display the extracted spectroscopic data (transitions, energy levels, etc.) and the extracted collisional data. The current features of the SPECTCOL tool are described in a forthcoming publication.

11. Conclusions

BASECOL2023 gives a wide overview of the field of inelastic rate coefficients, mostly for collisions with heavy projectiles and in the temperature range relevant to the ISM, circumstellar atmospheres, and cometary atmospheres. The numerical data sent by the producers of data are not modified. The producers of data have the right to modify the entries prior to their publication, and even later, as the BASECOL versioning system allows us to keep track of the changes at a fine granularity. BASECOL is one of the 40 interconnected databases of the VAMDC e-infrastructure, which ensures that the data can be easily identified and combined, for example by the SPECTCOL tool, with spectroscopic data from other databases such as the CDMS database (Endres et al. 2016) in order to produce ready-to-use outputs for the modelling of non-LTE media. Users can use the VAMDC standards and the java or python libraries in order to create their own access to BASECOL and to other databases in VAMDC.

From a scientific point of view, our main plan for the future is to maintain and further expand this database including new datasets, which is a challenge in itself. In addition, we plan to introduce technical changes that will, for example, allow the user to select data formats when exporting data and make it easier for data producers to prepare files. However, this idea is still in the making, and once implemented, it will be communicated to the astronomical community.

Finally, we stress that the BASECOL database is an international database that is open to all data producers who have published inelastic rate coefficients that fit within the database format. As mentioned in the introduction, Dr O. Denis-Alpizar is the next manager of the BASECOL database.

Acknowledgements. BASECOL has been supported by the VAMDC consortium and by Paris Astronomical Data Center (PADC) from Paris Observatory. For this paper and for the scientific update of BASECOL2023 MLD thanks her collaborator and co-author Corinne Boursier (CB) for her scientific contributions and support, she has been a key motor for the completion of this work. MLD thanks Otoniel Denis-Alpizar for his decision to take over the scientific leadership of BASECOL, and Yaye Awa Ba and Nicolas Moreau for the long term collaboration and their continuous support to the technical platforms. MLD thanks two post-docs who contributed to the maintenance of the database: Dr Sarandis Marinakis and Dr Fabien Daniel, the latter has left the field of research. We are grateful to one of our co-author, Dr Isabelle Kleiner, for very helpful discussions on the spectroscopy of CH_3OH. The list of co-authors includes the scientific team who maintains the database content, the technical team who designed and maintains the technical platforms, the data providers who provided their data in the requested format, thus contributing to the numerical and text information of the BASECOL database and paper.

[15] https://personal.sron.nl/~vdtak/radex/index.shtml

[16] https://vamdc.org/activities/research/software/spectcol/

References

Abrahamsson, E., Krems, R. V., & Dalgarno, A. 2007, ApJ, 654, 1171
Albert, D., Antony, B. K., Ba, Y. A., et al. 2020, ATOMS, 8
Alexander, M. H. & Dagdigian, P. J. 1985, J. Chem. Phys., 83, 2191
Alexander, M. H., Rackham, E. J., & Manolopoulos, D. E. 2004, J. Chem. Phys., 121, 5221
Amor, M. A., Hammami, K., & Wiesenfeld, L. 2021, M. N. R. A. S., 506, 957
Avery, L. W. & Green, S. 1989, ApJ, 337, 306
Ba, Y.-A., Dubernet, M.-L., Moreau, N., & Zwölf, C. M. 2020, Atoms, 8
Balakrishnan, N., Forrey, R. C., & Dalgarno, A. 1999a, ApJ, 514, 520
Balakrishnan, N., Vieira, M., Babb, J. F., et al. 1999b, ApJ, 524, 1122
Balakrishnan, N., Yan, M., & Dalgarno, A. 2002, ApJ, 568, 443
Balança, C. & Dayou, F. 2017, M. N. R. A. S., 469, 1673
Balança, C., Dayou, F., Faure, A., Wiesenfeld, L., & Feautrier, N. 2018, M. N. R. A. S., 479, 2692–2701
Balança, C., Quintas-Sánchez, E., Dawes, R., et al. 2021, M. N. R. A. S., 508, 1148
Balança, C., Scribano, Y., Loreau, J., Lique, F., & Feautrier, N. 2020, M. N. R. A. S., 495, 2524
Barinovs, G. & van Hemert, M. 2004, Chem. Phys. Lett., 399, 406
Barinovs, Ğ., van Hemert, M. C., Krems, R., & Dalgarno, A. 2005, ApJ, 620, 537
Ben Abdallah, D., Hammami, K., Najar, F., et al. 2008, ApJ, 686, 379
Ben Abdallah, D., Najar, F., Jaidane, N., Dumouchel, F., & Lique, F. 2012, M. N. R. A. S., 419, 2441
Ben Khalifa, M., Dagdigian, P., & Loreau, J. 2023, M. N. R. A. S., 253, 2577
Ben Khalifa, M., Dagdigian, P. J., & Loreau, J. 2022, J. Phys. Chem. A, 126, 9658
Ben Khalifa, M. & Loreau, J. 2021, M. N. R. A. S., 508, 1908
Bergeat, A., Chefdeville, S., Costes, M., et al. 2018, Nature Chemistry, 10, 519
Bian, W. & Werner, H.-J. 2000, J. Chem. Phys., 112, 220
Boothroyd, A. I., Keogh, W. J., Martin, P. G., & Peterson, M. R. 1996, J. Chem. Phys., 104, 7139
Bop, C., Kalugina, Y., & Lique, F. 2022a, J. Chem. Phys., 156, 204311
Bop, C. T. 2019, M. N. R. A. S., 487, 5685
Bop, C. T., Batista-Romero, F. A., Faure, A., et al. 2019a, ACS Earth and Space Chemistry, 3, 1151
Bop, C. T., Faye, N., & Hammami, K. 2019b, Chem. Phys., 519, 21
Bop, C. T., Faye, N. A. B., & Hammami, K. 2018, M. N. R. A. S., 478, 4410
Bop, C. T., Hammami, K., & Faye, N. A. B. 2017, M. N. R. A. S., 470, 2911
Bop, C. T., Hammami, K., Niane, A., Faye, N. A. B., & Jaïdane, N. 2016, M. N. R. A. S., 465, 1137
Bop, C. T., Khadri, F., & Hammami, K. 2022b, M. N. R. A. S., 518, 3533
Bop, C. T., Lique, F., Faure, A., Quintas-Sánchez, E., & Dawes, R. 2021, M. N. R. A. S., 501, 1911
Bouhafs, N., Lique, F., Faure, A., et al. 2017a, J. Chem. Phys., 146, 064309
Bouhafs, N., Rist, C., Daniel, F., et al. 2017b, M. N. R. A. S., 470, 2204
Boursier, C., Mandal, B., Babikov, D., & Dubernet, M. L. 2020, M. N. R. A. S., 498, 5489
Cabrera-González, L., Mera-Adasme, R., Páez-Hernández, D., & Denis-Alpizar, O. 2018, M. N. R. A. S., 480, 4969
Cabrera-González, L., Páez-Hernández, D., & Denis-Alpizar, O. 2020, M. N. R. A. S., 494, 129
Cecchi-Pestellini, C., Bodo, E., Balakrishnan, N., & Dalgarno, A. 2002, ApJ, 571, 1015
Cernicharo, J., Agúndez, M., Cabezas, C., et al. 2022, A&A, 657, L16
Cernicharo, J., Spielfiedel, A., Balança, C., et al. 2011, A&A, 531, A103
Chandra, S. & Kegel, W. H. 2000, Astron. Astrophys. Sup., 142, 113
Chefai, A., Ben Khalifa, M., Khadri, F., & Hammami, K. 2021, Phys. Chem. Chem. Phys., 23, 23741
Chefai, A., Jellali, C., Hammami, K., & Aroui, H. 2018, Astrophysics and Space Science, 363, 265
Corey, G. C. & McCourt, F. R. 1983, J. Chem. Phys., 87, 2723

Cybulski, S. M., Krems, R. V., Sadeghpour, H. R., et al. 2005, J. Chem. Phys., 122, 094307
Cybulski, S. M., Toczylowski, R. R., Lee, H.-S., & McCoy, A. B. 2000, J. Chem. Phys., 113, 9549
Dagdigian, P. 2018a, M. N. R. A. S., 479, 3227
Dagdigian, P. 2018b, J. Chem. Phys., 148, 024304
Dagdigian, P. J. 2020a, M. N. R. A. S., 494, 5239
Dagdigian, P. J. 2020b, M. N. R. A. S., 498, 5361
Dagdigian, P. J. 2020c, J. Chem. Phys., 152, 074307
Dagdigian, P. J. 2020d, J. Chem. Phys., 152, 224304
Dagdigian, P. J. 2021a, M. N. R. A. S., 505, 1987
Dagdigian, P. J. 2021b, M. N. R. A. S., 508, 118
Dagdigian, P. J. 2021c, Mol. Phys., 119
Dagdigian, P. J. 2022a, M. N. R. A. S., 518, 5976
Dagdigian, P. J. 2022b, J. Chem. Phys., 157, 104305
Dagdigian, P. J. & Alexander, M. H. 2013, J. Chem. Phys., 139, 194309
Dagdigian, P. J., Kłos, J., Warehime, M., & Alexander, M. H. 2016, J. Chem. Phys., 145, 164309
Danby, G., Flower, D. R., Kochanski, E., Kurdi, L., & Valiron, P. 1986, J. Phys. B: At. Mol. Opt. Phys., 19, 2891
Danby, G., Flower, D. R., Valiron, P., Kochanski, E., & Kurdi, L. 1987, J. Phys. B: At. Mol. Opt. Phys., 20, 1039
Danby, G., Flower, D. R., Valiron, P., Schilke, P., & Walmsley, C. M. 1988, M. N. R. A. S., 235, 229
Daniel, F., Dubernet, M.-L., & Grosjean, A. 2011, A&A, 536, A76
Daniel, F., Dubernet, M.-L., & Meuwly, M. 2004, J. Chem. Phys., 121, 4540
Daniel, F., Dubernet, M.-L., Meuwly, M., Cernicharo, J., & Pagani, L. 2005, M. N. R. A. S., 363, 1083
Daniel, F., Dubernet, M.-L., Pacaud, F., & Grosjean, A. 2010, A&A, 517, A13
Daniel, F., Faure, A., Dagdigian, P. J., et al. 2015, M. N. R. A. S., 446, 2312
Daniel, F., Faure, A., Wiesenfeld, L., et al. 2014, M. N. R. A. S., 444, 2544
Daniel, F., Rist, C., Faure, A., et al. 2016, M. N. R. A. S., 457, 1535
Dayou, F. & Balança, C. 2006, A&A, 459, 297
Demes, S., Lique, F., Faure, A., & Rist, C. 2020, The Journal of Chemical Physics, 153, 094301, publisher: AIP Publishing, LLC
Demes, S., Lique, F., Faure, A., & van der Tak, F. F. S. 2022, Monthly Notices of the Royal Astronomical Society, 518, 3593
Demes, S., Lique, F., Faure, A., et al. 2021, Monthly Notices of the Royal Astronomical Society, 509, 1252
Demes, S., Lique, F., Loreau, J., & Faure, A. 2023, M. N. R. A. S., 524, 2368
Denis-Alpizar, O., Inostroza, N., & Castro Palacio, J. 2018a, M. N. R. A. S., 473, 1438
Denis-Alpizar, O., Kalugina, Y., Stoecklin, T., Vera, M. H., & Lique, F. 2013, J. Chem. Phys., 139, 224301
Denis-Alpizar, O., Quintas-Sánchez, E., & Dawes, R. 2022, M. N. R. A. S., 512, 5546
Denis-Alpizar, O. & Rubayo-Soneira, J. 2019, M. N. R. A. S., 486, 1255
Denis-Alpizar, O. & Stoecklin, T. 2015, M. N. R. A. S., 451, 2986
Denis-Alpizar, O., Stoecklin, T., Dutrey, A., & Guilloteau, S. 2020, M. N. R. A. S., 497, 4276
Denis-Alpizar, O., Stoecklin, T., Guilloteau, S., & Dutrey, A. 2018b, M. N. R. A. S., 478, 1811
Denis-Alpizar, O., Stoecklin, T., & Halvick, P. 2014, J. Chem. Phys., 140, 084316
Denis-Alpizar, O., Stoecklin, T., Halvick, P., Dubernet, M.-L., & Marinakis, S. 2012, J. Chem. Phys., 137, 234301
Denis-Alpizar, O., Trabelsi, T., Hochlaf, M., & Stoecklin, T. 2018c, M. N. R. A. S., 475, 783
Desrousseaux, B., Coppola, C. M., Kazandjian, M. V., & Lique, F. 2018, J. Phys. Chem. A, 122, 8390
Desrousseaux, B. & Lique, F. 2018, M. N. R. A. S., 476, 4719
Desrousseaux, B. & Lique, F. 2020, J. Chem. Phys., 152, 074303
Desrousseaux, B., Lique, F., Goicoechea, J. R., Quintas-Sánchez, E., & Dawes, R. 2021, A&A, 645, A8
Desrousseaux, B., Quintas-Sánchez, E., Dawes, R., & Lique, F. 2019, J. Phys. Chem. A, 123, 9637
Dubernet, M., Berriman, G., Barklem, P., et al. 2023, in Proceedings IAU Symposium No. 371, Busan Korea, 9-11 August 2022, D. Soderblom & G. Nave eds., "Honoring Charlotte Moore Sitterly: Astronomical Spectroscopy in the 21st century", Cambridge University Press, International Astronomical Union 2023, Vol. S371, 72–84
Dubernet, M.-L., Alexander, M. H., Ba, Y. A., et al. 2013, Astr. Astroph., 553, A50
Dubernet, M. L., Antony, B. K., Ba, Y. A., et al. 2016, J. Phys. B: At. Mol. Opt. Phys., 49
Dubernet, M. L., Boudon, V., Culhane, J. L., et al. 2010, J. Quant. Spectrosc. Radiat. Transfer, 111, 2151
Dubernet, M.-L., Daniel, F., Grosjean, A., & Lin, C. Y. 2009, A&A, 497, 911
Dubernet, M.-L. & Quintas-Sánchez, E. 2019, Molecular Astrophysics, 16, 100046
Dubernet, M.-L., Quintas-Sánchez, E., & Tuckey, P. 2015, J. Chem. Phys., 143
Dumouchel, F., Faure, A., & Lique, F. 2010, M. N. R. A. S., 406, 2488
Dumouchel, F., Kłos, J., & Lique, F. 2011, Phys. Chem. Chem. Phys., 13, 8204
Dumouchel, F., Lique, F., Spielfiedel, A., & Feautrier, N. 2017, M. N. R. A. S., 471, 1849
Dumouchel, F., Spielfiedel, A., Senent, M., & Feautrier, N. 2012, Chem. Phys. Lett., 533, 6
Endres, C. P., Schlemmer, S., Schilke, P., Stutzki, J., & Mueller, H. S. P. 2016, J. of Mol. Spectrosc., 327, 95
Faure, A., Crimier, N., Ceccarelli, C., et al. 2007a, A&A, 472, 1029
Faure, A., Gorfinkiel, J. D., & Tennyson, J. 2004, M. N. R. A. S., 347, 323
Faure, A. & Josselin, E. 2008, A&A, 492, 257
Faure, A., Lique, F., & Loreau, J. 2020, M. N. R. A. S., 493, 776
Faure, A., Lique, F., & Wiesenfeld, L. 2016, M. N. R. A. S., 460, 2103
Faure, A. & Tennyson, J. 2001, M. N. R. A. S., 325, 443
Faure, A. & Tennyson, J. 2003, M. N. R. A. S., 340, 468
Faure, A., Varambhia, H. N., Stoecklin, T., & Tennyson, J. 2007b, M. N. R. A. S., 382, 840
Faure, A., Wiesenfeld, L., Scribano, Y., & Ceccarelli, C. 2012, M. N. R. A. S., 420, 699
Flower, D. R. 1999a, J. Phys. B: At. Mol. Opt. Phys., 32, 1755
Flower, D. R. 1999b, M. N. R. A. S., 305, 651
Flower, D. R. 2001a, J. Phys. B: At. Mol. Opt. Phys., 34, 2731
Flower, D. R. 2001b, M. N. R. A. S., 328, 147
Flower, D. R. & Lique, F. 2015, M. N. R. A. S., 446, 1750
Flower, D. R. & Roueff, E. 1998a, J. Phys. B: At. Mol. Opt. Phys., 31, 2935
Flower, D. R. & Roueff, E. 1998b, J. Phys. B: At. Mol. Opt. Phys., 31, L955
Flower, D. R. & Roueff, E. 1999a, M. N. R. A. S., 309, 833
Flower, D. R. & Roueff, E. 1999b, J. Phys. B: At. Mol. Opt. Phys., 32, 3399
Flower, D. R., Roueff, E., & Zeippen, C. J. 1998, J. Phys. B: At. Mol. Opt. Phys., 31, 1105
Forrey, R. C., Balakrishnan, N., Dalgarno, A., & Lepp, S. 1997, ApJ, 489, 1000
Franz, J., Mant, B. P., González-Sánchez, L., Wester, R., & Gianturco, F. A. 2020, J. Chem. Phys., 152, 234303
García-Vázquez, R. M., Márquez-Mijares, M., Rubayo-Soneira, J., & Denis-Alpizar, O. 2019, A&A, 631, A86
Garrison, B. J. & Lester, W. A. 1975, J. Chem. Phys., 63, 1449
Gianturco, F. A., González-Sánchez, L., Mant, B. P., & Wester, R. 2019, J. Chem. Phys., 151, 144304
Godard Palluet, A., Thibault, F., & Lique, F. 2022, J. Chem. Phys., 156, 104303
Goicoechea, J. R., Lique, F., & Santa-Maria, M. G. 2022, A&A, 658, A28
González-Sánchez, L., Mant, B. P., Wester, R., & Gianturco, F. A. 2020, ApJ, 897, 75
González-Sánchez, L., Yurtsever, E., Mant, B. P., Wester, R., & Gianturco, F. A. 2021, Phys. Chem. Chem. Phys., Advance Article
Gordon, I., Rothman, L., Hargreaves, R., et al. 2022, J. Quant. Spectrosc. Radiat. Transfer, 277, 107949
Gordon, R. G. & Kim, Y. S. 1972, J. Chem. Phys., 56, 3122
Green, S. 1975, ApJ, 201, 366
Green, S. 1989, ApJS, 70, 813
Green, S. 1991, ApJS, 76, 979
Green, S. 1994, ApJ, 434, 188
Green, S. 1995, ApJS, 100, 213
Green, S. & Chapman, S. 1978, ApJS, 37, 169
Green, S., Defrees, D. J., & McLean, A. D. 1987, ApJS, 65, 175
Green, S., Maluendes, S., & McLean, A. D. 1993, ApJS, 85, 181
Green, S. & Thaddeus, P. 1974, ApJ, 191, 653
Groenenboom, G. C. & Struniewicz, I. M. 2000, J. Chem. Phys., 113, 9562
Guillon, G. & Stoecklin, T. 2012, M. N. R. A. S., 420, 579
Hammami, K., Jaidane, N., Spielfiedel, A., & Feautrier, N. 2004, J. Chem. Phys., 121, 1325
Hammami, K., Lique, F., Jaïdane, N., et al. 2007, A&A, 462, 789
Hammami, K., Nkem, C., Owono Owono, L. C., Jaidane, N., & Ben Lakhdar, Z. 2008, J. Chem. Phys., 129, 204305
Hammami, K., Owono Owono, L., Jaidane, N., & Ben Lakhdar, Z. 2008a, J. Mol. Struct.: THEOCHEM, 853, 18
Hammami, K., Owono Owono, L. C., Jaidane, N. J., & Ben Lakhdar, Z. 2008b, J. Mol. Struct.: THEOCHEM, 860, 45
Hammami, K., Owono Owono, L. C., & Stäuber, P. 2009, A&A, 507, 1083
Heijmen, T. G. A., Moszynski, R., Wormer, P. E. S., & van der Avoird, A. 1997, J. Chem. Phys., 107, 9921
Herbst, E., Messer, J., De Lucia, F., & Helminger, P. 1984, J. of Mol. Spectrosc., 108, 42
Hernández, M. I., Tejeda, G., Fernández, J. M., & Montero, S. 2021, A&A, 647, A155
Hernández Vera, M., Kalugina, Y., Denis-Alpizar, O., Stoecklin, T., & Lique, F. 2014, J. Chem. Phys., 140, 224302
Hernández Vera, M., Lique, F., Dumouchel, F., Hily-Blant, P., & Faure, A. 2017, M. N. R. A. S., 468, 1084

Hernández Vera, M., Lique, F., Dumouchel, F., et al. 2013, M. N. R. A. S., 432, 468
Higgins, K. & Klemperer, W. 1999, J. Chem. Phys., 110, 1383
Hodges, M. P. & Wheatley, R. J. 2001, J. Chem. Phys., 114, 8836
Hougen, J., Kleiner, I., & Godefroid, M. 1994, J. of Mol. Spectrosc., 163, 559
Jankowski, P. & Szalewicz, K. 1998, J. Chem. Phys., 108, 3554
Jankowski, P. & Szalewicz, K. 2005, J. Chem. Phys., 123, 104301
Jaquet, R., Staemmler, V., Smith, M. D., & Flower, D. R. 1992, J. Phys. B: At. Mol. Opt. Phys., 25, 285
Kalemos, A., Mavridis, A., & Metropoulos, A. 1999, J. Chem. Phys., 111, 9536
Kalugina, Y., Alpizar, O. D., Stoecklin, T., & Lique, F. 2012, Phys. Chem. Chem. Phys., 14, 16458
Kalugina, Y., Kłos, J., & Lique, F. 2013, J. Chem. Phys., 139, 074301
Kalugina, Y. & Lique, F. 2015, M. N. R. A. S., 446, L21
Kalugina, Y., Lique, F., & Kłos, J. 2012, M. N. R. A. S., 2545
Kalugina, Y., Lique, F., & Marinakis, S. 2014, Phys. Chem. Chem. Phys., 16, 13500
Kalugina, Y. N., Faure, A., van der Avoird, A., Walker, K., & Lique, F. 2018, Phys. Chem. Chem. Phys., 20, 5469
Keller, H.-M., Floethmann, H., Dobbyn, A. J., et al. 1996, J. Chem. Phys., 105, 4983
Khadri, F., Chefai, A., & Hammami, K. 2020, M. N. R. A. S., 498, 5159
Khadri, F., Chefai, A., & Hammami, K. 2022a, M. N. R. A. S., 513, 4573
Khadri, F., Elabidi, H., & Hammami, K. 2023, M. N. R. A. S., 522, 4038
Khadri, F., Hachani, L., Elabidi, H., & Hammami, K. 2022b, M. N. R. A. S., 513, 6152
Khadri, F. & Hammami, K. 2019, Phys. Chem. Chem. Phys., 21, 4606
Kłos, J., Chalasinski, G., Berry, M. T., Bukowski, R., & Cybulski, S. M. 2000, J. Chem. Phys., 112, 2195
Kłos, J. & Lique, F. 2008, M. N. R. A. S., 390, 239
Kłos, J. & Lique, F. 2011, M. N. R. A. S., 418, 271
Kłos, J., Lique, F., & Alexander, M. H. 2007, Chem. Phys. Lett., 445, 12
Kłos, J., Lique, F., & Alexander, M. H. 2008, Chem. Phys. Lett., 455, 1
Kłos, J., Lique, F., & Alexander, M. H. 2009, Chem. Phys. Lett., 476, 135
Kłos, J., Dagdigian, P., & Lique, F. 2020a, M. N. R. A. S., 501, L38
Kłos, J., Dagdigian, P. J., Alexander, M. H., Faure, A., & Lique, F. 2020b, M. N. R. A. S., 493, 3491
Kłos, J., Ma, Q., Alexander, M. H., & Dagdigian, P. J. 2017a, J. Chem. Phys., 146
Kłos, J., Ma, Q., Dagdigian, P. J., et al. 2017b, M. N. R. A. S., 471, 4249
Lanza, M., Kalugina, Y., Wiesenfeld, L., Faure, A., & Lique, F. 2014a, M. N. R. A. S., 443, 3351
Lanza, M., Kalugina, Y., Wiesenfeld, L., & Lique, F. 2014b, J. Chem. Phys., 140, 064316
Lanza, M. & Lique, F. 2012, M. N. R. A. S., 424, 1261
Lanza, M. & Lique, F. 2014, J. Chem. Phys., 141, 164321
Launay, J. M. & Roueff, E. 1977, A&A, 56, 289
Lee, H., McCoy, A. B., Toczyłowski, R. R., & Cybulski, S. M. 2000, J. Chem. Phys., 113, 5736
Li, G., Werner, H.-J., Lique, F., & Alexander, M. H. 2007, J. Chem. Phys., 127, 174302
Li, H., Roy, P. N., & Le Roy, R. J. 2010, J. Chem. Phys., 133, 104305
Li, J. & Guo, H. 2014, Phys. Chem. Chem. Phys., 16, 6753
Lim, A. J., Rabadán, I., & Tennyson, J. 1999, M. N. R. A. S., 306, 473
Lique, F. 2010, J. Chem. Phys., 132, 044311
Lique, F., Daniel, F., Pagani, L., & Feautrier, N. 2015, M. N. R. A. S., 446, 1245
Lique, F., Dubernet, M.-L., Spielfiedel, A., & Feautrier, N. 2006a, A&A, 450, 399
Lique, F. & Faure, A. 2017, M. N. R. A. S., 472, 738
Lique, F., Honvault, P., & Faure, A. 2012, J. Chem. Phys., 137, 154303
Lique, F. & Kłos, J. 2011, M. N. R. A. S., 413, L20
Lique, F., Kłos, J., & Hochlaf, M. 2010a, Phys. Chem. Chem. Phys., 12, 15672
Lique, F., Kłos, J., Alexander, M. H., Le Picard, S. D., & Dagdigian, P. J. 2017, M. N. R. A. S., 474, 2313
Lique, F., Kłos, J., & Le Picard, S. D. 2018, Phys. Chem. Chem. Phys., 20, 5427
Lique, F., Senent, M.-L., Spielfiedel, A., & Feautrier, N. 2007, J. Chem. Phys., 126, 164312
Lique, F. & Spielfiedel, A. 2007, A&A, 462, 1179
Lique, F., Spielfiedel, A., & Cernicharo, J. 2006b, A&A, 451, 1125
Lique, F., Spielfiedel, A., Dhont, G., & Feautrier, N. 2006c, A&A, 458, 331
Lique, F., Spielfiedel, A., Dubernet, M.-L., & Feautrier, N. 2005, J. Chem. Phys., 123, 134316
Lique, F., Spielfiedel, A., Feautrier, N., et al. 2010b, J. Chem. Phys., 132, 024303
Loreau, J., Faure, A., & Lique, F. 2022, M. N. R. A. S., 516, 5964
Loreau, J., Kalugina, Y. N., Faure, A., van der Avoird, A., & Lique, F. 2020, J. Chem. Phys., 153, 214301
Loreau, J., Lique, F., & Faure, A. 2018, Ap. J. (Letters), 853, L5
Ma, Q., Kłos, J., Alexander, M. H., van der Avoird, A., & Dagdigian, P. J. 2014, J. Chem. Phys., 141, 174309
Machin, L. & Roueff, E. 2005, J. Phys. B: At. Mol. Opt. Phys., 38, 1519
Machin, L. & Roueff, E. 2006, A&A, 460, 953
Machin, L. & Roueff, E. 2007, A&A, 465, 647
Maluendes, S., McLean, A. D., & Green, S. 1992, J. Chem. Phys., 96, 8150
Mandal, B. & Babikov, D. 2023a, A&A, 678, A51
Mandal, B. & Babikov, D. 2023b, A&A, 671, A51
Mandal, B., Joy, C., Bostan.D., Eng, A., & Babikov, D. 2022, J.of Phys. Chem. Letters, 14, 817
Mant, B. P., Gianturco, F. A., González-Sánchez, L., Yurtsever, E., & Wester, R. 2020a, J. Phys. B: At. Mol. Opt. Phys., 53, 025201
Mant, B. P., Gianturco, F. A., Wester, R., Yurtsever, E., & González-Sánchez, L. 2020b, Phys. Rev. A, 102, 062810
Mant, B. P., Gianturco, F. A., Wester, R., Yurtsever, E., & González-Sánchez, L. 2020c, J. Int. Mass Spectrom., 457, 116426
Mant, B. P., Yurtsever, E., González-Sánchez, L., Wester, R., & Gianturco, F. A. 2021, J. Chem. Phys., 154, 084305
Maret, S., Faure, A., Scifoni, E., & Wiesenfeld, L. 2009, M. N. R. A. S., 399, 425
Marinakis, S., Dean, I. L., Kłos, J., & Lique, F. 2015, Phys. Chem. Chem. Phys., 17, 21583
Marinakis, S., Kalugina, Y., Kłos, J., & Lique, F. 2019, A&A, 629, A130
Mielke, S. L., Garrett, B. C., & Peterson, K. A. 2002, J. Chem. Phys., 116, 4142
Monteiro, T. 1984, M. N. R. A. S., 210, 1
Monteiro, T. S. 1985, M. N. R. A. S., 214, 419
Monteiro, T. S. & Stutzki, J. 1986, M. N. R. A. S., 221, 33P
Moszynski, R., Wormer, P. E. S., Jeziorski, B., & van der Avoird, A. 1994, J. Chem. Phys., 101, 2811
Muchnick, P. & Russek, A. 1994, J. Chem. Phys., 100, 4336
Müller, H. S. P., Schlöder, F., Stutzki, J., & Winnewisser, G. 2005, J. of Mol. Struct., 742, 215
Murdachaew, G., Szalewicz, K., Jiang, H., & Bačić, Z. 2004, J. Chem. Phys., 121, 11839
Najar, F., Ben Abdallah, D., Spielfiedel, A., et al. 2014, Chem. Phys. Lett., 614, 251
Najar, F., Nouai, M., ElHanini, H., & Jaidane, N. 2017, M. N. R. A. S., 472, 2919–2925
Ndaw, D., Bop, C. T., Dieye, G., Faye, N. B., & Lique, F. 2021, M. N. R. A. S., 503, 5976
Neufeld, D. A. & Green, S. 1994, ApJ, 432, 158
Nkem, C., Hammami, K., Manga, A., et al. 2009, J. Mol. Struct.: THEOCHEM, 901, 220
Nolte, J. L., Stancil, P. C., Lee, T.-G., Balakrishnan, N., & Forrey, R. C. 2011, ApJ, 744, 62
Offer, A. R., Hemert, M. C. v., & Dishoeck, E. F. v. 1994, J. Chem. Phys., 100, 362
Pagani, L., Bourgoin, A., & Lique, F. 2012, A&A, 548, L4
Palma, A. 1987, ApJS, 64, 565
Palma, A. & Green, S. 1987, ApJ, 316, 830
Palma, A., Green, S., Defrees, D. J., & McLean, A. D. 1988, J. Chem. Phys., 89, 1401
Parlant, G. & Yarkony, D. R. 1999, J. Chem. Phys., 110, 363
Patkowski, K., Brudermann, J., Steinbach, C., Buck, U., & Moszynski, R. 2002, J. Chem. Phys., 117, 11166
Patkowski, K., Cencek, W., Jankowski, P., et al. 2008, J. Chem. Phys., 129, 094304
Pearson, J. C., Mueller, H. S. P., Pickett, H. M., Cohen, E. A., & Drouin, B. J. 2010, J. Quant. Spectrosc. Radiat. Transfer, 111, 1614
Phillips, T. R., Maluendes, S., & Green, S. 1996, ApJS, 107, 467
Phillips, T. R., Maluendes, S., McLean, A. D., & Green, S. 1994, J. Chem. Phys., 101, 5824
Pirlot Jankowiak, P., Lique, F., & Dagdigian, P. 2023a, M. N. R. A. S., 523, 3732
Pirlot Jankowiak, P., Lique, F., & Dagdigian, P. J. 2023b, M. N. R. A. S., 526, 885
Pottage, J. T., Flower, D. R., & Davis, S. L. 2002, J. Phys. B: At. Mol. Opt. Phys., 35, 2541
Pottage, J. T., Flower, D. R., & Davis, S. L. 2004, M. N. R. A. S., 352, 39
Price, T. J., Forrey, R. C., Yang, B., & Stancil, P. C. 2021, J. Chem. Phys., 154
Quintas-Sánchez, E., Dawes, R., & Denis-Alpizar, O. 2021, Mol. Phys., 119, e1980234
Quintas-Sánchez, E. & Dubernet, M.-L. 2017, Phys. Chem. Chem. Phys., 19, 6849
Rabadan, I., Sarpal, B. K., & Tennyson, J. 1998, M. N. R. A. S., 299, 171
Rabli, D. & Flower, D. R. 2010a, M. N. R. A. S., 406, 95
Rabli, D. & Flower, D. R. 2010b, M. N. R. A. S., 403, 2033
Rabli, D. & Flower, D. R. 2011, M. N. R. A. S., 411, 2011
Ramachandran, C., De Fazio, D., Cavalli, S., Tarantelli, F., & Aquilanti, V. 2009, Chem. Phys. Lett., 469, 26
Ramachandran, R., Kłos, J., & Lique, F. 2018, J. Chem. Phys., 148, 084311
Reese, C., Stoecklin, T., Voronin, A., & Rayez, J. C. 2005, A&A, 430, 1139
Rinnenthal, J. L. & Gericke, K.-H. 2002, J. Chem. Phys., 116, 9776
Roueff, E. & Flower, D. R. 1999, M. N. R. A. S., 305, 353

Roueff, E. & Zeippen, C. J. 1999, A&A, 343, 1005
Roueff, E. & Zeippen, C. J. 2000, Astron. Astrophys. Sup., 142, 475
Sahnoun, E., Ben Khalifa, M., Khadri, F., & Hammami, K. 2020, Ap. S. S., 365, 1
Sahnoun, E., Nkem, C., Naindouba, A., et al. 2018, Astrophysics and Space Science, 363, 195
Santander, C., Denis-Alpizar, O., & Cárdenas, C. 2022, A&A, 657, A55
Sarpal, B. K. & Tennyson, J. 1993, M. N. R. A. S., 263, 909
Sarrasin, E., Abdallah, D. B., Wernli, M., et al. 2010, M. N. R. A. S., 404, 518
Schewe, H. C., Ma, Q., Vanhaecke, N., et al. 2015, J. Chem. Phys., 142, 204310
Schröder, K., Staemmler, V., Smith, M. D., Flower, D. R., & Jaquet, R. 1991, J. Phys. B: At. Mol. Opt. Phys., 24, 2487
Schwenke, D. W. 1988, J. Chem. Phys., 89, 2076
Scribano, Y., Faure, A., & Lauvergnat, D. 2012, J. Chem. Phys., 136, 094109
Song, L., Balakrishnan, N., van der Avoird, A., Karman, T., & Groenenboom, G. C. 2015a, J. Chem. Phys., 142, 204303
Song, L., Balakrishnan, N., Walker, K. M., et al. 2015b, ApJ, 813, 96
Song, L., van der Avoird, A., & Groenenboom, G. C. 2013, J. Phys. Chem. A, 117, 7571
Spielfiedel, A., Feautrier, N., Najar, F., et al. 2012, M. N. R. A. S., 421, 1891
Spielfiedel, A., Feautrier, N., Najar, F., et al. 2013, M. N. R. A. S., 429, 923
Spielfiedel, A., Senent, M.-L., Dayou, F., et al. 2009, J. Chem. Phys., 131, 014305
Spielfiedel, A., Senent, M. L., Kalugina, Y., et al. 2015, J. Chem. Phys., 143, 024301
Staemmler, V. & Flower, D. R. 1991, J. Phys. B: At. Mol. Opt. Phys., 24, 2343
Stoecklin, T., Denis-Alpizar, O., & Halvick, P. 2015, M. N. R. A. S., 449, 3420
Stoecklin, T. & Voronin, A. 2011, J. Chem. Phys., 134, 204312
Stoecklin, T., Voronin, A., & Rayez, J. C. 2003, Chem. Phys., 294, 117
Tennyson, J. & Faure, A. 2019, in Gas-phase chemistry in space: from elementary particles to complex organic molecules, ed. F. Lique & A. Faure, AAS-IOP Astronomy
Toboła, R., Dumouchel, F., Kłos, J., & Lique, F. 2011, J. Chem. Phys., 134, 024305
Toboła, R., Kłos, J., Lique, F., Chałasiński, G., & Alexander, M. H. 2007, A&A, 468, 1123
Toboła, R., Lique, F., Kłos, J., & Chałasiński, G. 2008, J. Phys. B: At. Mol. Opt. Phys., 41, 155702
Toczyłowski, R. R., Doloresco, F., & Cybulski, S. M. 2001, J. Chem. Phys., 114, 851
Tonolo, F., Bizzocchi, L., Melosso, M., et al. 2021, J. Chem. Phys., 155, 234306
Tonolo, F., Lique, F., Melosso, M., Puzzarini, C., & Bizzocchi, L. 2022, M. N. R. A. S., 516, 2653
Troscompt, N., Faure, A., Wiesenfeld, L., Ceccarelli, C., & Valiron, P. 2009, A&A, 493, 687
Turner, B. E., Chan, K.-W., Green, S., & Lubowich, D. A. 1992, ApJ, 399, 114
Turpin, F., Stoecklin, T., & Voronin, A. 2010, A&A, 511, A28
Urzúa-Leiva, R. & Denis-Alpizar, O. 2020, ACS Earth and Space Chemistry, 4, 2384
Valiron, P., Wernli, M., Faure, A., et al. 2008, J. Chem. Phys., 129, 134306
van der Tak, F. F. S., Lique, F., Faure, A., Black, J. H., & van Dishoeck, E. F. 2020a, Atoms, 8, 15
van der Tak, F. F. S., Lique, F., Faure, A., Black, J. H., & van Dishoeck, E. F. 2020b, Atoms, 8
Varambhia, H. N., Gupta, M., Faure, A., Baluja, K. L., & Tennyson, J. 2009, J. Phys. B: At. Mol. Opt. Phys., 42, 095204
Vieira, D. & Krems, R. V. 2017, The Astrophysical Journal, 835, 255
Vincent, L. F. M., Spielfiedel, A., & Lique, F. 2007, A&A, 472, 1037
Walker, K. M., Dumouchel, F., Lique, F., & Dawes, R. 2016, J. Chem. Phys., 145, 024314
Walker, K. M., Lique, F., & Dawes, R. 2018, M. N. R. A. S., 473, 1407
Walker, K. M., Lique, F., Dumouchel, F., & Dawes, R. 2017, M. N. R. A. S., 466, 831
Walker, K. M., Song, L., Yang, B. H., et al. 2015, ApJ, 811, 27
Wan, Y., Balakrishnan, N., Yang, B. H., Forrey, R. C., & Stancil, P. C. 2019, M. N. R. A. S., 488, 381
Wernli, M., Valiron, P., Faure, A., et al. 2006, A&A, 446, 367
Wernli, M., Wiesenfeld, L., Faure, A., & Valiron, P. 2007a, A&A, 464, 1147
Wernli, M., Wiesenfeld, L., Faure, A., & Valiron, P. 2007b, A&A, 475, 391
Xu, L.-H., Fisher, J., Lees, R. M., et al. 2008, JOURNAL OF MOLECULAR SPECTROSCOPY, 251, 305
Yang, B. & Stancil, P. C. 2014, ApJ, 783, 92
Yang, B., Stancil, P. C., Balakrishnan, N., & Forrey, R. C. 2010, ApJ, 718, 1062
Yang, B., Stancil, P. C., Kimura, M., Satomi, W., & Nagao, M. 2013, ApJ, 765, 77
Yang, B., Walker, K. M., Forrey, R. C., Stancil, P. C., & Balakrishnan, N. 2015a, A&A, 578, A65
Yang, B., Zhang, P., Qu, C., et al. 2020, Chem. Phys., 532, 110695
Yang, B., Zhang, P., Qu, C., et al. 2018a, Phys. Chem. Chem. Phys., 20, 28425
Yang, B., Zhang, P., Qu, C., et al. 2018b, J. Phys. Chem. A, 122, 1511
Yang, B. H., Zhang, P., Wang, X. H., et al. 2015b, Nature Communications, 6, 6629
Yang, B. H., Zhang, P., Wang, X. H., et al. 2016, J. Chem. Phys., 145, 034308
Yau, A. W. & Dalgarno, A. 1976, ApJ, 206, 652
Zeng, T., Li, H., Le Roy, R. J., & Roy, P. N. 2011, J. Chem. Phys., 135, 094304
Żółtowski, M., Lique, F., Karska, A., & Żuchowski, P. S. 2021, M. N. R. A. S., 502, 5356

[1] Observatoire de Paris, PSL University, Sorbonne Université, CNRS, LERMA, Paris, France
[2] Univ. Bordeaux, CNRS, Bordeaux INP, ISM, UMR 5255, F-33400 Talence, France
[3] Facultad de Ingeniería, Universidad Autónoma de Chile, Av. Pedro de Valdivia 425, 7500912 Providencia, Santiago, Chile
[4] LSAMA, Department of Physics, Faculty of Sciences, Université Tunis El-Manar, 1060 Tunis, Tunisia
[5] Marquette University, Chemistry Department, Milwaukee, WI 53233, USA
[6] Department of Chemistry and Biochemistry, University of Nevada, Las Vegas, NV 89154, USA
[7] KU Leuven, Department of Chemistry, Celestijnenlaan 200F, 3001 Leuven, Belgium
[8] Univ Rennes, CNRS, IPR (Institut de Physique de Rennes) - UMR 6251, F-35000 Rennes, France
[9] Department of Chemistry, The University of Manchester, Oxford Road, Manchester M13 9PL, UK
[10] Departamento de Física, Facultad de Ciencias, Universidad de Chile, Av. Las Palmeras 3425, Ñuñoa, Santiago, Chile
[11] Centro para el Desarrollo de la Nanociencia y la Nanotecnología (CEDENNA), Av. Ecuador 3493, Santiago 9170124, Chile
[12] Department of Chemistry, The Johns Hopkins University, Baltimore, MD 21218-2685, USA
[13] LOMC - UMR 6294, CNRS-Université du Havre,25 rue Philippe Lebon, BP 1123, F-76063 Le Havre Cedex, France
[14] IPAG, Université Grenoble Alpes & CNRS, CS 40700, F-38058 Grenoble, France
[15] Department of Physics, Penn State University, Berks Campus, Reading, PA 19610, USA
[16] Department of Theoretical Physics and Quantum Informatics, Faculty of Applied Physics and Mathematics, Gdansk University of Technology, ul. Narutowicza 11/12, 80-233 Gdansk, Poland
[17] Institute for Ion Physics and Applied Physics, University of Innsbruck, Technikerstr. 25/3, 6020 Innsbruck, Austria
[18] Department of Chemistry, University of Patras, Patras GR-26504,Greece
[19] Departamento de Química Física, University of Salamanca, Plaza de los Caídos s/n, 37008 Salamanca, Spain
[20] Theoretical Chemistry, Institute for Molecules and Materials, Radboud University, Heyendaalseweg 135, 6525 AJ Nijmegen, The Netherlands
[21] Université Paris Cité and Univ Paris Est Creteil, CNRS, LISA, F-75013 Paris, France
[22] Joint Quantum Institute, Department of Physics, University of Maryland, College Park, Maryland 20742, USA
[23] Department of Physics, Temple University, Philadelphia, Pennsylvania 19122, USA
[24] Laboratoire Atomes Lasers, Département de Physique, Faculté des Sciences et Techniques, Université Cheikh Anta Diop, Dakar, 5005, Senegal
[25] Depart. of Physics and Astronomy and Center for Simulational Physics, The University of Georgia, Athens, Georgia 30602-2451, USA
[26] Departamento de Física Atómica y Molecular, Instituto Superior de Tecnologías y Ciencias Aplicadas, Universidad de La Habana. Ave. Salvador Allende No. 1110, 10400 Plaza de la Revolución, La Habana, Cuba
[27] Department of Chemistry, Missouri University of Science and Technology, Rolla, MO 65409, USA
[28] Physical Research Laboratory, Ahmedabad, India

[29] Department of Physics and Astronomy, University College London, London WC1E 6BT, UK
[30] Scuola Normale Superiore, Piazza dei Cavalieri 7, I-56126 Pisa, Italy
[31] Department of Chemistry "Giacomo Ciamician," University of Bologna, Via F. Selmi 2, I-40126 Bologna, Italy
[32] Department of Chemistry, Koç University, Rumelifeneri Yolu, Sariyer, TR-34450, Istanbul, Turkey

Appendix A: List of VAMDC cases and BASECOL associated molecules

Table A1. List of BASECOL2023 molecules with the associated cases.

Cases	Description	Molecules
dcs	Diatomic cs	$^{36}ArH^+$, $^{36}ArD^+$, AlO^+, CF^+, CH^+, CN^-, CO, CS
		H_2, HD, HeH^+, HCl, HF, KCl, NaH, NeH^+, NO^+, NS^+, PN, SiH^+, SiO, SiS
hunda	Diatomic os: hund's case a	CH ($X^2\Pi$), OH ($X^2\Pi$) , OD ($X^2\Pi$), NO ($X^2\Pi$), SH ($X^2\Pi$), C_6H ($X^2\Pi$)
hundb[a]	Diatomic os: hund's case b	C_2^- ($X^2\Sigma_g^+$), CN ($X^2\Sigma^+$), ^{13}CN ($X^2\Sigma^+$), $C^{15}N$ ($X^2\Sigma^+$), CO^+ ($X^2\Sigma^+$)
		C_4 ($X^3\Sigma_g^-$), H_2^+ ($X^2\Sigma_g^+$), NH ($X^3\Sigma^+$), O_2 ($X^3\Sigma_g^-$), SO ($X\ ^3\Sigma^-$)
ltcs	linear triatomic cs	AlCN, AlNC, C_3, C_2H^-, CO_2, HCN, HNC, DCN, DNC, HCO^+, $HC^{17}O^+$, DCO^+,
		HCP, HCS^+, N_2H^+, OCS
nltcs	non-linear triatomic cs	D_2O, HDO, H_2O, H_2S, SiC_2, SO_2
stcs	symmetric top cs	H_3^+, H_3O^+, NH_3, ND_3, CH_3CN, CH_3NC, CH_3OH
lpcs	linear polyatomic cs	CNCN, C_6H^-, HC_3N, HCCNC, HNCCC, HMgNC, $NCCNH^+$, C_3O, C_3S, C_4H^- , C_5, C_5O, C_5S
asymcs	asymmetric cs	H_2CO, $HOCO^+$, C_3H_2, NH_2D, ND_2H
asymos	asymmetric os	none
sphcs	spherical cs	none
sphos	spherical os	none
ltos	linear triatomic os	C_2H ($X^2\Sigma^+$), C_2D ($X^2\Sigma^+$), C_2N^- ($X^3\Sigma^-$), C_2O($X^3\Sigma^-$), MgCN ($X^2\Sigma^+$), MgNC ($X^2\Sigma^+$)
lpos	linear polyatomic os	none
nltos	non-linear triatomic os	NH_2 (X^2B_1), CH_2 (X^3B_1), HCO

Notes. cs and os denote closed shell and open shell molecules. The molecules in blue have issues with the case assignment; this is explained in the text (see Section 2.3). [(a)] T he hundb case includes intermediate coupling based on Hund's case b.

Appendix B: Tables of collisional datasets

This appendix provides tables describing the content of the BASECOL database. The names of the columns are self-explanatory, and each line in the sections corresponds to collisional dataset(s), as described in our technical publication. The current tables display some differences compared to Table 1 of the BASECOL2012 publication. The internal ID is not provided anymore because BASECOL2023 stores the successive versions of a given collisional dataset, and each version has a different ID. It is still possible to navigate through BASECOL with the IDs if the user keeps them in memory, as one ID corresponds to a unique couple collisional dataset/version. To date, we have removed the output flat files corresponding to the combination of collisional and spectroscopic data from the BASECOL interface; therefore, the tables do not include information related to those output files. In the following tables, the columns provide the following information: (1) the atomic or molecular target; (2) the perturbing projectile; (3) the energy levels for which rate coefficients are available: the symbols r, f, v, rv, rt, and h are used to denote rotational, fine, vibrational, ro-vibrational, ro-torsional, and hyperfine transitions, respectively (for example, r7 means that rate coefficients are available for the 7 lowest rotational levels); (4) temperature range in kelvin for which the rates have been calculated; (5 & 6) references to the papers describing, respectively, the collisional calculations and the potential energy surfaces; and (7) the year of publication. For Section 5, columns (2) and (6) have been removed. In the tables, the notation o/p-H_2 is a synthetic notation that corresponds to two datasets that have the same characteristics: number (except if marked otherwise) and type of levels, temperature range, and references; however one dataset is for a collision with ortho-H_2, and the other one with para-H_2.

Appendix B.1: Collisional data with electrons

Table B1. List of collisional data with electrons.

Target	Levels	T (K)	Ref	Year
		RECOMMENDED		
CH^+	r8	100-15000	Lim et al. (1999)	1999
H_2^+	v3	100-20000	Sarpal & Tennyson (1993)	1993
o/p-H_2^+	r2	100-10000	Faure & Tennyson (2001)	2001
o/p-H_3^+	r2/r4	100-10000	Faure & Tennyson (2003)	2003
o/p-H_3O^+	r4/r8	100-10000	Faure & Tennyson (2003)	2003
HeH^+	r3	100-20000	Rabadan et al. (1998)	1998
HeH^+	v3	100-20000	Rabadan et al. (1998)	1998
CO^+	r5	100-10000	Faure & Tennyson (2001)	2001
HCO^+	r3	100-10000	Faure & Tennyson (2001)	2001
NO^+	r5	100-10000	Faure & Tennyson (2001)	2001
o/p-H_2O	r18	100-8000	Faure et al. (2004)	2004
o/p-D_2O	r18	100-8000	Faure et al. (2004)	2004
o-H_2O	rv411	200 - 5000	Faure & Josselin (2008)	2008
p-H_2O	rv413	200 - 5000	Faure & Josselin (2008)	2008
HDO	r36 (a-type)	100-8000	Faure et al. (2004)	2004
HDO	r36 (b-type)	100-8000	Faure et al. (2004)	2004
HCN	r9	5-2000	Faure et al. (2007b)	2007
HCN	h10	10-100-1000	Faure et al. (2007b)	2007
HNC	r9	5-2000	Faure et al. (2007b)	2007
HNC	h10	10-1000	Faure et al. (2007b)	2007
DCN	r9	5-2000	Faure et al. (2007b)	2007
DCN	h10	10-100-1000	Faure et al. (2007b)	2007
DNC	r9	5-2000	Faure et al. (2007b)	2007
DNC	h10	10-100-1000	Faure et al. (2007b)	2007
SiO	r41	5-5000	Varambhia et al. (2009)	2009

Notes. This list of datasets has not changed since 2012 (see text).

Appendix B.2: Collisional data of atoms excited by heavy projectiles

Table B2. List of collisional datasets of atoms and atomic ions/cations excited by heavy projectiles.

Target	Projectile	Levels	T (K)	Ref	PES Ref	Year
			RECOMMENDED			
C	H	f3	5-1000	Abrahamsson et al. (2007)	Kalemos et al. (1999)	2007
C	o/p-H_2	f3	10-1200	Schröder et al. (1991)	Schröder et al. (1991)	1991
C	**He**	f3	5-350	Bergeat et al. (2018)	Bergeat et al. (2018)	2018
C^+	H	f2	20-2000	Barinovs et al. (2005)	Barinovs & van Hemert (2004)	2005
C^+	**o/p-H_2**	f2	5-500	Kłos et al. (2020a)	Kłos et al. (2020a)	2020
O	**H**	f3	50-1000	Vieira & Krems (2017)	Parlant & Yarkony (1999)	2017
O	**H**	f3	10-1000	Lique et al. (2017)	Dagdigian et al. (2016)	2017
O	**He**	f3	10-1000	Lique et al. (2017)	Lique et al. (2017)	2017
O	**o/p-H_2**	f3	10-1000	Lique et al. (2017)	Dagdigian et al. (2016)	2017
Si	**He**	f3	5-1000	Lique et al. (2018)	Lique et al. (2018)	2018
S	**He**	f3	5-1000	Lique et al. (2018)	Lique et al. (2018)	2018
Si^+	H	f2	20-2000	Barinovs et al. (2005)	Barinovs et al. (2005)	2005
			NOT RECOMMENDED **(outdated)**			
O	H	f3	50-1000	Launay & Roueff (1977)	Launay & Roueff (1977)	1977
O	H	f3	50-1000	Abrahamsson et al. (2007)	Parlant & Yarkony (1999)	2007
O	o/p-H_2	f3	20-1500	Jaquet et al. (1992)	Jaquet et al. (1992)	1992
C	H	f3	4-1000	Launay & Roueff (1977)	Yau & Dalgarno (1976)	1977
C	He	f3	10-150	Staemmler & Flower (1991)	Staemmler & Flower (1991)	1991

Notes. The species in bold correspond to the systems added since 2012.

Appendix B.3: Collisional data of diatomic species excited by heavy projectiles

Table B3. List of neutral and ionic diatomic collisional data.

Target	Coll.	Levels	T (K)	Ref	PES Ref	Year
			RECOMMENDED			
AlO^+	**He**	r16	10-1005	Denis-Alpizar et al. (2018c)	Denis-Alpizar et al. (2018c)	2018
$^{36}ArH^+$	**He**	r11	5-300	Bop et al. (2016)	Bop et al. (2016)	2016
$^{36}ArH^+$	**He**	rv33	10-500	García-Vázquez et al. (2019)	García-Vázquez et al. (2019)	2019
$^{36}ArD^+$	**He**	r13	10-500	García-Vázquez et al. (2019)	García-Vázquez et al. (2019)	2019
C_2^-	**He**	r9	5-100	Mant et al. (2020a)	Mant et al. (2020a)	2020
C_2^-	**Ar**	r5	5-100	Mant et al. (2020c)	Mant et al. (2020c)	2020
C_2^-	**Ne**	r5	5-100	Mant et al. (2020c)	Mant et al. (2020c)	2020
C_2^-	**He**	v3	5-100	Mant et al. (2020b)	Mant et al. (2020b)	2020
C_2^-	**Ne**	v3	5-100	Mant et al. (2020b)	Mant et al. (2020b)	2020
C_2^-	**Ar**	v3	5-100	Mant et al. (2020b)	Mant et al. (2020b)	2020
CF^+	**He**	r22	5-155	Denis-Alpizar et al. (2018a)	Denis-Alpizar et al. (2018a)	2019
CF^+	**He**	h29	5-155	Denis-Alpizar et al. (2018a)	Denis-Alpizar et al. (2018a)	2019
CF^+	**p-H_2**	r21	10-300	Denis-Alpizar et al. (2019)	Denis-Alpizar et al. (2019)	2019
CF^+	**p-H_2**	r22	5-150	Desrousseaux et al. (2021)	Desrousseaux et al. (2019)	2021
CF^+	**o-H_2**	r22	5-150	Desrousseaux et al. (2021)	Desrousseaux et al. (2019)	2021
CH^+	He	r11	20-2000	Hammami et al. (2009)	Hammami et al. (2008a)	2009
CH^+	He	r6	0.1-200	Turpin et al. (2010)	Turpin et al. (2010)	2010
CH	**He**	f30	10-300	Marinakis et al. (2015)	Marinakis et al. (2015)	2015
CH	**He**	h60	10-300	Marinakis et al. (2019)	Marinakis et al. (2015)	2019
CN^-	o/p-H_2[c]	r11	5-100	Kłos & Lique (2011)	Kłos & Lique (2011)	2011
CN^-	**He**	r11	5-100	González-Sánchez et al. (2020)	González-Sánchez et al. (2020)	2020
CN^-	**Ar**	r11	5-100	González-Sánchez et al. (2021)	González-Sánchez et al. (2021)	2021
CN^-	**He**	v3	5-100	Mant et al. (2021)	Mant et al. (2021)	2021
CN	He	f41	5 - 350	Lique et al. (2010b)	Lique et al. (2010b)	2010
CN	He	h37	5 - 30	Lique & Kłos (2011)	Lique et al. (2010b)	2011
CN[a]	**p-H_2**	r18	5 - 300	Kalugina et al. (2013)	Kalugina et al. (2013)	2013
CN	**o-H_2**	r16	5 - 300	Kalugina et al. (2013)	Kalugina et al. (2013)	2013
CN[b]	**p-H_2**	f25	5 - 100	Kalugina et al. (2013)	Kalugina et al. (2013)	2013
CN[c]	**p-H_2**	f17	5 - 100	Kalugina et al. (2013)	Kalugina et al. (2013)	2013
CN	**o-H_2**	f17	5 - 100	Kalugina et al. (2013)	Kalugina et al. (2013)	2013
CN	**o/p-H_2**	h73	5 - 100	Kalugina & Lique (2015)	Kalugina et al. (2013)	2015
^{13}CN	**p-H_2**	h146	5 - 80	Flower & Lique (2015)	Kalugina et al. (2013)	2015
$C^{15}N$	**p-H_2**	h34	5 - 150	Flower & Lique (2015)	Kalugina et al. (2013)	2015
CO	He	r15	5-500	Cecchi-Pestellini et al. (2002)	Heijmen et al. (1997)	2002
CO	He	v7	500-5000	Cecchi-Pestellini et al. (2002)	Heijmen et al. (1997)	2002
CO	**H**	r77	2-3000	Walker et al. (2015)	Song et al. (2013)	2015
CO	H	r8	5-100	Balakrishnan et al. (2002)	Keller et al. (1996)	2002
CO	H	r17	100-3000	Balakrishnan et al. (2002)	Keller et al. (1996)	2002
CO	**H**	rv350	2-3000	Song et al. (2015b)	Song et al. (2013)	2015
CO	H	v5	100-3000	Balakrishnan et al. (2002)	Keller et al. (1996)	2002
CO	o/p-H_2	r41	1-3000	Yang et al. (2010)	Jankowski & Szalewicz (1998)	2010
CO	o/p-H_2	r6	5-70	Wernli et al. (2006)	Jankowski & Szalewicz (1998)	2006
CO	o-H_2	r20	5-400	Flower (2001a)	Jankowski & Szalewicz (1998)	2001
CO	p-H_2	r29	5-400	Flower (2001a)	Jankowski & Szalewicz (1998)	2001
CO	**p-H_2**	rv45	1-300	Yang et al. (2016)	Yang et al. (2015b)	2016
CO	**o-H_2**	rv29	1-300	Yang et al. (2016)	Yang et al. (2015b)	2016
CO	**o/p-t-H_20**	r11	10-100	Faure et al. (2020)	Kalugina et al. (2018)	2020
CS	He	r31	10-300	Lique et al. (2006b)	Lique et al. (2006b)	2006
CS	He	rv114	300-1500	Lique & Spielfiedel (2007)	Lique & Spielfiedel (2007)	2007
CS	**o/p-H_2**	rv42	5-1000	Yang et al. (2018a)	Yang et al. (2018a)	2018
CS	**o/p-H_2**	r30	5-305	Denis-Alpizar et al. (2018b)	Denis-Alpizar et al. (2012)	2018
HCl	**He**	r21	1-3000	Yang & Stancil (2014)	Murdachaew et al. (2004)	2014
HCl	**He**	r11	10-300	Lanza & Lique (2012)	Lanza & Lique (2012)	2012
HCl	**He**	h40	10-300	Lanza & Lique (2012)	Lanza & Lique (2012)	2012
HCl[a]	**p-H_2**	r11	10-300	Lanza et al. (2014a)	Lanza et al. (2014b)	2014
HCl	**o-H_2**	r11	10-300	Lanza et al. (2014a)	Lanza et al. (2014b)	2014
HCl	**o/p-H_2**	h20	10-300	Lanza & Lique (2014)	Lanza et al. (2014b)	2014

Continued on next page.

Table B3 – Continued from previous page.

Target	Coll.	Levels	T (K)	Ref	PES Ref	Year
HCl	**H**	r11	10-500	Lique & Faure (2017)	Bian & Werner (2000)	2017
HF	**He**	r21	1-3000	Yang et al. (2015a)	Moszynski et al. (1994)	2015
HF	He	r10	0.1-300	Reese et al. (2005)	Stoecklin et al. (2003)	2005
HF	**o/p-H_2**	r6	0.1-150	Guillon & Stoecklin (2012)	Guillon & Stoecklin (2012)	2012
HF	**H**	r9	10-500	Desrousseaux & Lique (2018)	Li et al. (2007)	2018
HF	**o/p-t-$H_2$0**	r7	10-150	Loreau et al. (2022)	Loreau et al. (2020)	2022
HD	He	r10	80-2000	Roueff & Zeippen (1999)	Muchnick & Russek (1994)	1999
HD	**He**	rv94	2-100	Nolte et al. (2011)	Muchnick & Russek (1994)	2011
HD	**He**	rv223	2-1000	Nolte et al. (2011)	Muchnick & Russek (1994)	2011
HD	**o/p-H_2**	r9	1-10000	Wan et al. (2019)	Patkowski et al. (2008)	2019
HD	o/p-H_2	rv24	100-1940	Flower & Roueff (1999a)	Schwenke (1988)	1999
HD	**H**	r11	10-1000	Desrousseaux et al. (2018)	Mielke et al. (2002)	2018
HD	H	r10	100-2000	Roueff & Flower (1999)	Boothroyd et al. (1996)	1999
HD	H	rv30	100-2080	Flower & Roueff (1999a)	Boothroyd et al. (1996)	1999
o-H_2	He	rv23	100-6000	Flower et al. (1998)	Muchnick & Russek (1994)	1998
p-H_2	He	rv26	100-6000	Flower et al. (1998)	Muchnick & Russek (1994)	1998
o-H_2	o-H_2	rv17	100-6000	Flower & Roueff (1999b)	Schwenke (1988)	1999
p-H_2	o-H_2	rv19	100-6000	Flower & Roueff (1999b)	Schwenke (1988)	1999
o-H_2	p-H_2	rv23	100-6000	Flower & Roueff (1998a)	Schwenke (1988)	1998
p-H_2	p-H_2	rv26	100-6000	Flower & Roueff (1998a)	Schwenke (1988)	1998
H_2	**H**	r9	300-1500	Lique et al. (2012)	Mielke et al. (2002)	2012
o/p-H_2	H	r3	100-1000	Forrey et al. (1997)	Boothroyd et al. (1996)	1997
o-H_2	H	rv23	100-6000	Flower & Roueff (1998b)	Boothroyd et al. (1996)	1998
p-H_2	H	rv26	100-6000	Flower & Roueff (1998b)	Boothroyd et al. (1996)	1998
HeH^+	**H**	r10	5-500	Desrousseaux & Lique (2020)	Ramachandran et al. (2009)	2020
KCl	**p-H_2**	r16	2-50	Sahnoun et al. (2018)	Sahnoun et al. (2018)	2018
NaH	**He**	r11	5-200	Bop et al. (2019b)	Bop et al. (2019b)	2019
NeH^+	**He**	r11	5-300	Bop et al. (2017)	Bop et al. (2017)	2017
NH	He	f25	5- 350	Toboła et al. (2011)	Cybulski et al. (2005)	2011
NH	**He**	f25	10- 350	Ramachandran et al. (2018)	Ramachandran et al. (2018)	2018
NO^+	**He**	r8	1-205	Denis-Alpizar & Stoecklin (2015)	Stoecklin & Voronin (2011)	2015
NO^+	**p-H_2**	r19	5-300	Cabrera-González et al. (2020)	Cabrera-González et al. (2020)	2020
NO	**He**	f98	10-500	Kłos et al. (2008)	Kłos et al. (2000)	2008
NO	**p-H_2**	h100	7-100	Ben Khalifa & Loreau (2021)	Kłos et al. (2017a)	2021
NS^+	**He**	r28	10-305	Cabrera-González et al. (2018)	Cabrera-González et al. (2018)	2018
NS^+	**He**	h40	10-305	Cabrera-González et al. (2018)	Cabrera-González et al. (2018)	2018
NS^+	**o/p-H_2**	r15	5-50	Bop et al. (2022a)	Bop et al. (2022a)	2019
NS^+	**p-H_2**	r24	5-100	Bop (2019)	Bop (2019)	2019
NS^+	**p-H_2**	h67	10-100	Bop (2019)	Bop (2019)	2019
OH	He	f46	5-350	Kłos et al. (2007)	Lee et al. (2000)	2007
OH	**He**	f44	5-350	Kalugina et al. (2014)	Kalugina et al. (2014)	2014
OH	**He**	h56	5-350	Marinakis et al. (2019)	Kalugina et al. (2014)	2019
OH	**o/p-H_2**	f20	10-150	Kłos et al. (2017b)	Ma et al. (2014)	2017
OH	**o/p-H_2**	h24	10-150	Kłos et al. (2020b)	Ma et al. (2014)	2020
OD	**o/p-H_2**	h40	5-200	Dagdigian (2021a)	Ma et al. (2014)	2021
OH	**H**	h24	5-500	Dagdigian (2022a)	Alexander et al. (2004)	2022
O_2	He	f36	5-350	Lique (2010)	Groenenboom et al. (2000)	2010
O_2	**o/p-H_2**	r7	5-150	Kalugina et al. (2012)	Kalugina et al. (2012)	2012
PN	He	r31	10-300	Toboła et al. (2007)	Toboła et al. (2007)	2007
PN	**p-H_2**	r40	10-300	Najar et al. (2017)	Najar et al. (2017)	2017
SH	He	f60	5-350	Kłos et al. (2009)	Cybulski et al. (2000)	2009
SiH^+	He	r11	5-200	Nkem et al. (2009)	Nkem et al. (2009)	2009
SiO	**He**	r27	10-300	Dayou & Balança (2006)	Dayou & Balança (2006)	2006
SiO	**He**	rv246	250-10000	Balança & Dayou (2017)	Balança & Dayou (2017)	2017
SiO	**o/p-H_2**	rv47	5-1000	Yang et al. (2018b)	Yang et al. (2018b)	2018
SiO[d]	**o/p-H_2**	r21	5-300	Balança et al. (2018)	Balança et al. (2018)	2018
SiO[e]	**o/p-H_2**	r30	5-1000	Balança et al. (2018)	Balança et al. (2018)	2018
SiS	He	r26	10-200	Vincent et al. (2007)	Vincent et al. (2007)	2007
SiS	He	rv505	100-1500	Toboła et al. (2008)	Toboła et al. (2008)	2008
SiS	o/p-H_2	r41	5-300	Kłos & Lique (2008)	Kłos & Lique (2008)	2008
SO	He	f31	5-50	Lique et al. (2005)	Lique et al. (2005)	2005

Continued on next page.

Table B3 – Continued from previous page.

Target	Coll.	Levels	T (K)	Ref	PES Ref	Year
SO	He	f91	60-300	Lique et al. (2006a)	Lique et al. (2005)	2006
SO	He	rv236	300-800	Lique et al. (2006c)	Lique et al. (2006c)	2006
SO	o/p-H_2	rv273	5-3000	Price et al. (2021)	Yang et al. (2020)	2021
SO	p-H_2	r31	5-50	Lique et al. (2007)	Lique et al. (2007)	2007
			NOT RECOMMENDED **(outdated)**			
CH^+	He	r11	20-200	Hammami et al. (2008a)	Hammami et al. (2008a)	2008
CN	p-H_2	h73	5 - 100	Kalugina et al. (2012)	Kalugina et al. (2012)	2012
CS	p-H_2	r21	20-300	Turner et al. (1992)	Green & Chapman (1978)	1992
CS	p-H_2	r13	10-100	Green & Chapman (1978)	Green & Chapman (1978)	1978
HCl	He	r8	10-300	Neufeld & Green (1994)	Neufeld & Green (1994)	1994
HCl	He	h28	10-300	Neufeld & Green (1994)	Neufeld & Green (1994)	1994
HD	o/p-H_2	r9	50-500	Flower (1999a)	Schwenke (1988)	1999
SiO	p-H_2	r21	20-300	Turner et al. (1992)	Turner et al. (1992)	1992
SiO	p-H_2	r20	10-300	Dayou & Balança (2006)	Dayou & Balança (2006)	2006
SO	p-H_2	f70	50-350	Green (1994)	Green (1994)	1994

Notes. The species in bold correspond to the systems added since 2012.[(a)] The transitions among the first two levels of the projectile are provided. [(b)] In this dataset the projectile remains in its ground state. [(c)] The projectile's transitions j=2-2 and j=2-0 are provided. [(d)] This SiO dataset from Balança et al. (2018) uses the CC method. [(e)] This SiO dataset from Balança et al. (2018) uses the CS method.

Appendix B.4: Collisional data of triatomic species excited by heavy projectiles

Table B4. List of triatomic collisional data.

Target	Coll.	Levels	T (K)	Ref	PES Ref	Year
			RECOMMENDED			
AlCN	**He**	r30	5-100	Hernández Vera et al. (2013)	Hernández Vera et al. (2013)	2013
AlNC	**He**	r30	5-100	Hernández Vera et al. (2013)	Hernández Vera et al. (2013)	2013
AlNC	**p-H_2**	r27	5-105	Urzúa-Leiva et al. (2020)	Urzúa-Leiva et al. (2020)	2020
C_3	He	r6	5-15	Ben Abdallah et al. (2008)	Ben Abdallah et al. (2008)	2008
C_3	**He**	rv23	10-155	Stoecklin et al. (2015)	Denis-Alpizar et al. (2014)	2015
C_3	**o/p-H_2**	r11	5-50	Santander et al. (2022)	Santander et al. (2022)	2022
C_2H	**He**	h46	5-100	Spielfiedel et al. (2013)	Spielfiedel et al. (2013)	2013
C_2H	**o/p-H_2**	f41	5-500	Pirlot Jankowiak et al. (2023b)	Dagdigian (2018b)	2023
C_2H	**o/p-H_2**	h38	5-100	Pirlot Jankowiak et al. (2023b)	Dagdigian (2018b)	2023
C_2D	**o/p-H_2**	f31	5-200	Pirlot Jankowiak et al. (2023b)	Dagdigian (2018b)	2023
C_2D	**o/p-H_2**	h55	5-100	Pirlot Jankowiak et al. (2023b)	Dagdigian (2018b)	2023
$C^{13}CH$	**p-H_2**	h98	5-100	Pirlot Jankowiak et al. (2023a)	Dagdigian (2018b)	2023
^{13}CCH	**p-H_2**	h98	5-100	Pirlot Jankowiak et al. (2023a)	Dagdigian (2018b)	2023
C_2H^-	**He**	r13	5-100	Dumouchel et al. (2012)	Dumouchel et al. (2012)	2012
C_2H^-	**He**	r9	5-100	Gianturco et al. (2019)	Dumouchel et al. (2012)	2019
C_2N^-	**He**	r16	5-100	Franz et al. (2020)	Franz et al. (2020)	2020
C_2O	**He**	f31	2-80	Khadri et al. (2022b)	Khadri et al. (2022b)	2022
o-CH_2	**o/p-H_2**	h69	5-300	Dagdigian (2021b)	Dagdigian (2021c)	2021
p-CH_2	**o/p-H_2**	r27	5-300	Dagdigian (2021b)	Dagdigian (2021c)	2021
CO_2	**He**	r21	4-300	Godard Palluet et al. (2022)	Godard Palluet et al. (2022)	2022
HCN	He	r26	5-500	Dumouchel et al. (2010)	Toczyłowski et al. (2001)	2010
HCN	**p-H_2**	r13	5-100	Hernández Vera et al. (2014)	Denis-Alpizar et al. (2013)	2014
HCN	**o/p-H_2**	r26	5-500	Hernández Vera et al. (2017)	Denis-Alpizar et al. (2013)	2017
HCN	**o/p-H_2**	h34	5 - 500	Goicoechea et al. (2022)	Denis-Alpizar et al. (2013)	2022
HCN	**p-t-$H_2$0**	r8	5 - 150	Dubernet et al. (2019)	Quintas-Sánchez et al. (2017)	2019
HNC	He	r26	5-500	[c]Dumouchel et al. (2010)	Sarrasin et al. (2010)	2010
HNC	o/p-H_2	r11	5-100	Dumouchel et al. (2011)	Dumouchel et al. (2011)	2011
HNC	**o/p-H_2**	r26	5-500	Hernández Vera et al. (2017)	Dumouchel et al. (2011)	2017
HCO^+	**He**	r6	5-100	Tonolo et al. (2021)	Tonolo et al. (2021)	2021
HCO^+	**o/p-H_2**	r22	10-200	Denis-Alpizar et al. (2020)	Denis-Alpizar et al. (2020)	2020
DCO^+	**p-H_2**	r22	10-200	Denis-Alpizar et al. (2020)	Denis-Alpizar et al. (2020)	2020
DCO^+	p-H_2	h31	5-300	Pagani et al. (2012)	Monteiro (1985)	2012
$HC^{17}O^+$	**p-H_2**	h33	5-100	Tonolo et al. (2022)	Tonolo et al. (2022)	2022
HCO	**o/p-H_2**	h86	5-200	Dagdigian (2020b)	Dagdigian (2020d)	2020
HCP	p-H_2	r11	10-70	Hammami et al. (2008)	Hammami et al. (2008)	2008

Continued on next page.

Table B4 – Continued from previous page.

Target	Coll.	Levels	T (K)	Ref	PES Ref	Year
HCP	He	r16	20-200	Hammami et al. (2008b)	Hammami et al. (2008b)	2008
HCS^+	**He**	r20	5-100	Dubernet et al. (2015)	Dubernet et al. (2015)	2015
HCS^+	**p-H_2**	r31	5-100	Denis-Alpizar et al. (2022)	Quintas-Sánchez et al. (2021)	2022
o/p-H_2O	**He**	r10	2-3000	Yang et al. (2013)	Patkowski et al. (2002)	1993
o/p-H_2O	He	r45	20-2000	Green et al. (1993)	Maluendes et al. (1992)	1993
p-H_2O	o/p-H_2	r45	5-1500	Daniel et al. (2011)	Valiron et al. (2008)	2011
o-H_2O	o-H_2	r45	5-1500	Daniel et al. (2011)	Valiron et al. (2008)	2011
o-H_2O	p-H_2	r45	5-1500	Dubernet et al. (2009)	Valiron et al. (2008)	2011
o/p-H_2O	**p-H_2**	r97	10-2000	Żółtowski et al. (2021)	Valiron et al. (2008)	2021
o/p-H_2O	o/p-t-H_2	r45	20-2000	Faure et al. (2007a)	Valiron et al. (2008)	2007
o/p-H_2O	t-H_2	rv411	200 - 5000	Faure & Josselin (2008)	Valiron et al. (2008)	2008
o/p-H_2O	**H**	r45	5-1500	Daniel et al. (2015)	Dagdigian & Alexander (2013)	2015
o/p-H_2O	**t-H_2O**	r59	100 - 800	Boursier et al. (2020)	Boursier et al. (2020)	2020
o/p-H_2O	**t-H_2O**	r21/r22	5 - 1000	Mandal & Babikov (2023a)	Jankowski & Szalewicz (2005)	2023
o/p-D_2O	**p-H_2**	r6	5-100	Faure et al. (2012)	Valiron et al. (2008)	2012
HDO	He	r34	50-500	Green (1989)	Palma et al. (1988)	1989
HDO	**p-t-H_2**	r30	5 - 300	Faure et al. (2012)	Valiron et al. (2008)	2012
HDO	**o-H_2**	r30	5 - 300	Faure et al. (2012)	Valiron et al. (2008)	2012
o/p-H_2S	**o/p-H_2**	r19	5 - 500	Dagdigian (2020a)	Dagdigian (2020c)	2020
MgCN	**He**	r36	5-100	Hernández Vera et al. (2013)	Hernández Vera et al. (2013)	2013
MgCN	**He**	f41	5-100	Hernández Vera et al. (2013)	Hernández Vera et al. (2013)	2013
MgNC	**He**	r36	5-100	Hernández Vera et al. (2013)	Hernández Vera et al. (2013)	2013
MgNC	**He**	f41	5-100	Hernández Vera et al. (2013)	Hernández Vera et al. (2013)	2013
o/p-NH_2	**o/p-H_2**	r15	10-150	Bouhafs et al. (2017a)	Li & Guo (2014)	1978
N_2H^+	He	r7	5-50	Daniel et al. (2005)	Daniel et al. (2004)	2005
N_2H^+	He	h55	5-50	Daniel et al. (2005)	Daniel et al. (2004)	2005
N_2H^+	**p-H_2**	r26	5-500	Balança et al. (2020)	Spielfiedel et al. (2015)	2020
N_2H^+	**p-H_2**	h64	5-70	Lique et al. (2015)	Spielfiedel et al. (2015)	2015
OCS	p-H_2	r13	10-100	Green & Chapman (1978)	Green & Chapman (1978)	1978
OCS	He	r27	10-150	Flower (2001b)	Higgins & Klemperer (1999)	2001
OCS	**Ar**	r21	5-400	Chefai et al. (2018)	Chefai et al. (2018)	2018
o-SiC_2	He	r40	25-125	Chandra & Kegel (2000)	Palma & Green (1987)	2000
SO_2	He	r50	25-125	Green (1995)	Palma (1987)	1995
SO_2	o/p-H_2	r31	5-30	Cernicharo et al. (2011)	Spielfiedel et al. (2009)	2011
NON-RECOMMENDED **(mostly outdated)**						
C_2H	**o/p-H_2**	h30	10-300	Dagdigian (2018a)	Dagdigian (2018b)	2018
C_2H	**p-H_2**	f17	5-80	Dumouchel et al. (2017)	Najar et al. (2014)	2017
C_2H	**p-H_2**	h34	2-80	Dumouchel et al. (2017)	Najar et al. (2014)	2017
C_2D	**p-H_2**	h49	2-80	Dumouchel et al. (2017)	Najar et al. (2014)	2017
C_2D	**p-H_2**	f17	5-80	Dumouchel et al. (2017)	Najar et al. (2014)	2017
HCN	He	h13	10-30	Monteiro & Stutzki (1986)	Green & Thaddeus (1974)	1986
HCN	He	r8	5-100	Green & Thaddeus (1974)	Green & Thaddeus (1974)	1974
HCN	p-H_2	h31	5 - 100	Ben Abdallah et al. (2012)	Ben Abdallah et al. (2012)	2012
HCO^+	p-H_2	r21	5-390	Flower (1999b)	Monteiro (1985)	1999
HCS^+	He	r11	10-60	Monteiro (1984)	Monteiro (1984)	1984
o/p-H_2O	o/p-H_2	r5	20-140	Phillips et al. (1996)	Phillips et al. (1994)	1996
N_2H^+	He	r7	5-40	Green (1975)	Green (1975)	1975

Notes. For H_2O collisional data: t-H_2, t-H_2O means that H_2, H_2O are thermalised over para and ortho species (you should refer to the papers to see how this is done); o/p-t-H_2 or o/p-t-H_2O means that H_2 or H_2O is thermalised over para-species only or ortho-species only. The species in bold correspond to the systems added since 2012.

Appendix B.5: Collisional data of species with more than 3 atoms excited by heavy projectiles

Table B5. List of collisional datasets for molecules with more than three atoms.

Target	Coll.	Levels	T (K)	Ref	PES Ref	Year
RECOMMENDED						
o/p c-C_3H_2	He	r47/48	30-120	Chandra & Kegel (2000)	Green et al. (1987)	2000
C_3O	**He**	r31	5-150	Bop et al. (2022b)	Khadri & Hammami (2019)	2022
C_3S	**He**	r11	2-25	Sahnoun et al. (2020)	Sahnoun et al. (2020)	2020
C_4	He	f30	5-50	Lique et al. (2010a)	Lique et al. (2010a)	2010
C_4H^-	**o/p-H_2**	r30	5-100	Balança et al. (2021)	Balança et al. (2021)	2021
C_5	**He**	r15	5-300	Chefai et al. (2021)	Chefai et al. (2021)	2021
C_5H^+	**He**	r16	5-100	Khadri et al. (2023)	Khadri et al. (2023)	2023
C_5O	**He**	r31	5-150	Bop et al. (2022b)	Khadri et al. (2022a)	2022
C_5S	**He**	r51	2-100	Khadri et al. (2020)	Khadri et al. (2020)	2020
C_6H	**He**	f122	5-100	Walker et al. (2018)	Walker et al. (2018)	2018
C_6H	**He**	h52	5-100	Walker et al. (2018)	Walker et al. (2018)	2018
C_6H^-	**He**	r11	5-100	Walker et al. (2017)	Walker et al. (2016)	2017
C_6H^-	**o/p-H_2**	r31	5-100	Walker et al. (2017)	Walker et al. (2016)	2017
p-CH_3CN	**He**	r75	7-100	Ben Khalifa et al. (2023)	Ben Khalifa et al. (2022)	2023
o-CH_3CN	**He**	r52	7-100	Ben Khalifa et al. (2023)	Ben Khalifa et al. (2022)	2023
p-CH_3NC	**He**	r63	7-100	Ben Khalifa et al. (2023)	Ben Khalifa et al. (2022)	2023
o-CH_3NC	**He**	r66	7-100	Ben Khalifa et al. (2023)	Ben Khalifa et al. (2022)	2023
A/E-CH_3OH	**He**	rt150	10-400	Rabli & Flower (2011)	Pottage et al. (2002)	2011
A-CH_3OH	**He**	r256, vt=0	10-200	Rabli & Flower (2010b)	Pottage et al. (2002)	2010
A-CH_3OH	**He**	r256, vt=1	10-200	Rabli & Flower (2010b)	Pottage et al. (2002)	2010
A-CH_3OH	**He**	r256, vt=2	10-200	Rabli & Flower (2010b)	Pottage et al. (2002)	2010
E-CH_3OH	**He**	r256, vt=0	10-200	Rabli & Flower (2010b)	Pottage et al. (2002)	2010
E-CH_3OH	**He**	r256, vt=1	10-200	Rabli & Flower (2010b)	Pottage et al. (2002)	2010
E-CH_3OH	**He**	r256, vt=2	10-200	Rabli & Flower (2010b)	Pottage et al. (2002)	2010
A-CH_3OH	**p-H_2**	r256, vt=0	10-200	Rabli & Flower (2010a)	Pottage et al. (2004)	2010
A-CH_3OH	**p-H_2**	r256, vt=1	10-200	Rabli & Flower (2010a)	Pottage et al. (2004)	2010
A-CH_3OH	**p-H_2**	r256, vt=2	10-200	Rabli & Flower (2010a)	Pottage et al. (2004)	2010
E-CH_3OH	**p-H_2**	r256, vt=0	10-200	Rabli & Flower (2010a)	Pottage et al. (2004)	2010
E-CH_3OH	**p-H_2**	r256, vt=1	10-200	Rabli & Flower (2010a)	Pottage et al. (2004)	2010
E-CH_3OH	**p-H_2**	r256, vt=2	10-200	Rabli & Flower (2010a)	Pottage et al. (2004)	2010
CNCN	**He**	r30	5-150	Ndaw et al. (2021)	Ndaw et al. (2021)	2021
o/p-H_2CO	He	r40/r41	10-300	Green (1991)	Garrison & Lester (1975)	1991
o-H_2CO	o/p-H_2	r10	5-100	Troscompt et al. (2009)	Troscompt et al. (2009)	2009
p-H_3O^+	**o/p-H_2**	r21	10-300	Demes et al. (2022)	Demes et al. (2020)	2022
o-H_3O^+	**o/p-H_2**	r11	10-300	Demes et al. (2022)	Demes et al. (2020)	2022
HC_3N	He	r11	10-40	Wernli et al. (2007a,b)	Wernli et al. (2007a,b)	2007
HC_3N	**o/p-H_2**	r38	10-300	Faure et al. (2016)	Wernli et al. (2007a)	2016
HC_3N	**t-p-H_2**	r38	10-300	Faure et al. (2016)	Wernli et al. (2007a)	2016
HC_3N	**o/p-H_2**	h61	10-100	Faure et al. (2016)	Wernli et al. (2007a)	2016
HC_3N	**t-p-H_2**	h61	10-100	Faure et al. (2016)	Wernli et al. (2007a)	2016
HNCCC	**o/p-H_2**	r30	5-80	Bop et al. (2021)	Bop et al. (2019a)	2021
HCCNC	**o/p-H_2**	r30	5-80	Bop et al. (2021)	Bop et al. (2019a)	2021
HMgNC	**He**	r14	5-200	Amor et al. (2021)	Amor et al. (2021)	2021
$HOCO^+$	He	r25	10-30	Hammami et al. (2007)	Hammami et al. (2004)	2007
$HNCCN^+$	**He**	r11	5-100	Bop et al. (2018)	Bop et al. (2018)	2018
o/p-NH_3	He	r22/16	5-300	Machin & Roueff (2005)	Hodges & Wheatley (2001)	2005
o/p-NH_3	**o/p-H_2**	r33/62	100-500	Demes et al. (2023)	Maret et al. (2009)	2023
o/p-NH_3	**p-t-H_2**	r33/62	100-500	Demes et al. (2023)	Maret et al. (2009)	2023
o/p-NH_3	**o/p-H_2**	r17/34	10-200	Bouhafs et al. (2017b)	Maret et al. (2009)	2017
o/p-NH_3	p-H_2	r6/10	5-100	Maret et al. (2009)	Maret et al. (2009)	2009
o/p-NH_3	**H**	r17/34	10-200	Bouhafs et al. (2017b)	Li & Guo (2014)	2017
o/p-NH_2D	He	r9	5-100	Machin & Roueff (2006)	Hodges & Wheatley (2001)[a]	2006
o/p-NH_2D	**p-H_2**	r79	5-300	Daniel et al. (2014)	Maret et al. (2009)	2014
o/p-ND_2H	He	r9	5-100	Machin & Roueff (2007)	Hodges & Wheatley (2001)[a]	2007
o/p-ND_2H	**p-H_2**	r16	5-50	Daniel et al. (2016)	Maret et al. (2009)	2016
o/p/meta-ND_3	**p-H_2**	r16/r9/r9	5-50	Daniel et al. (2016)	Maret et al. (2009)	2016
NON-RECOMMENDED **(mostly outdated)**						

Continued on next page.

Table B5 – Continued from previous page.

Target	Coll.	Levels	T (K)	Ref	PES Ref	Year
HC_3N	He	r21	10-80	Green & Chapman (1978)	Green & Chapman (1978)	1978
HC_3N	p-H_2	r51	10-100	Wernli et al. (2007a,b)	Wernli et al. (2007a,b)	2007
o-NH_3	p-H_2	r9	15-300	Danby et al. (1986)	Danby et al. (1986)	1986
p-NH_3	p-H_2	r16	15-300	Danby et al. (1987)	Danby et al. (1986)	1987
o/p-NH_3	p-H_2	r17/24	15-300	Danby et al. (1988)	Danby et al. (1986)	1988

Notes. The species in bold correspond to the systems added since 2012. [(a)] The PES of Hodges & Wheatley (2001) was adapted by Machin & Roueff (2006) and Machin & Roueff (2007) to account for the isotopic shift.

Appendix C: Figures

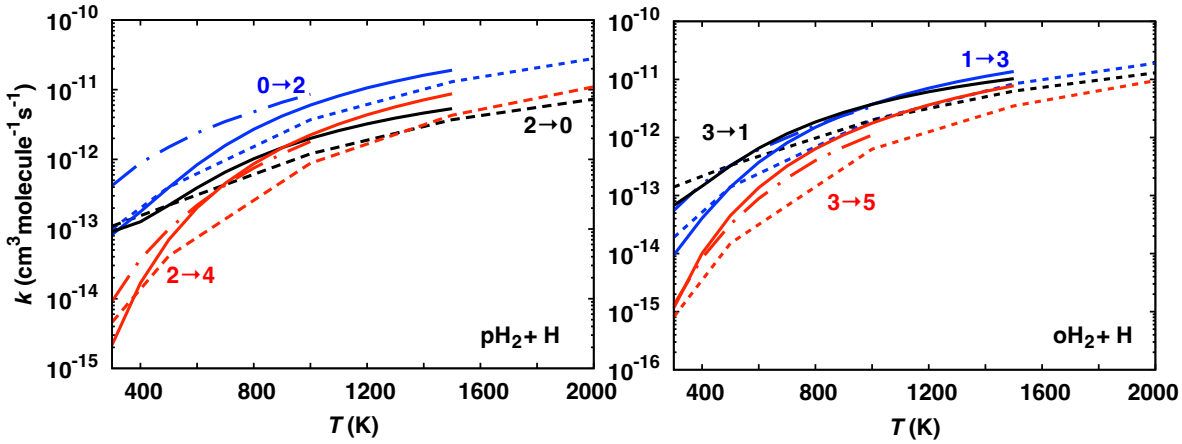

Fig. C.1. Rotational rate coefficients of para-H_2 and ortho-H_2 by H reported by Forrey et al. (1997) (dash-dotted lines), Flower & Roueff (1998b) (dashed lines), and Lique et al. (2012) (solid lines). Rotational transitions of H_2 are labelled as $j_i \rightarrow j_f$.

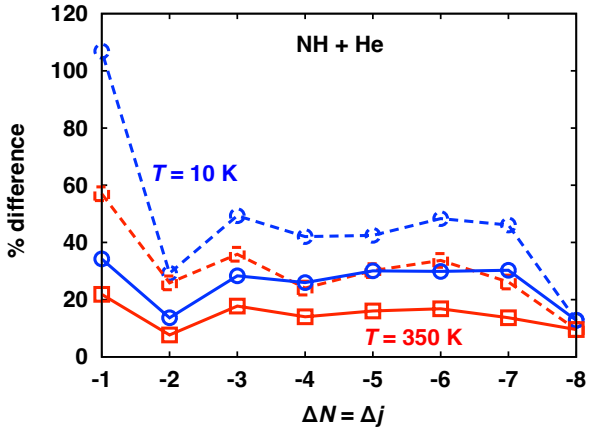

Fig. C.2. Average percentage difference (solid lines) and maximum percentage difference (dashed lines) between the rate coefficients reported by Toboła et al. (2011) and Ramachandran et al. (2018) for the $\Delta N = \Delta j$ transitions in the NH+He collision at 10 K (circles) and 350 K (squares).

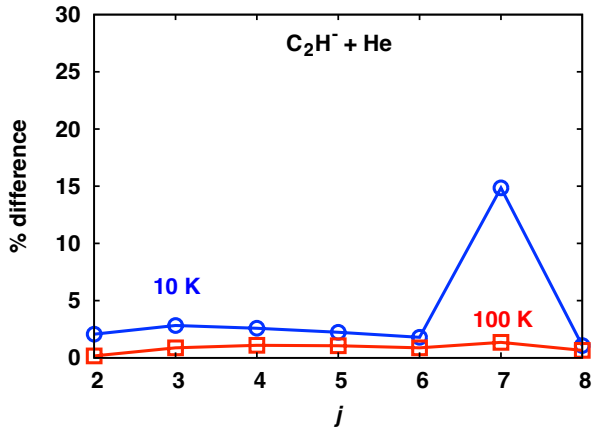

Fig. C.3. Percentage difference between rate coefficients reported by Dumouchel et al. (2012) and Gianturco et al. (2019) for the $\Delta j = 2$ transitions (strong propensity was found for this transition) in the C_2H^-+He collision at 10 K (circles) and 100 K (squares).

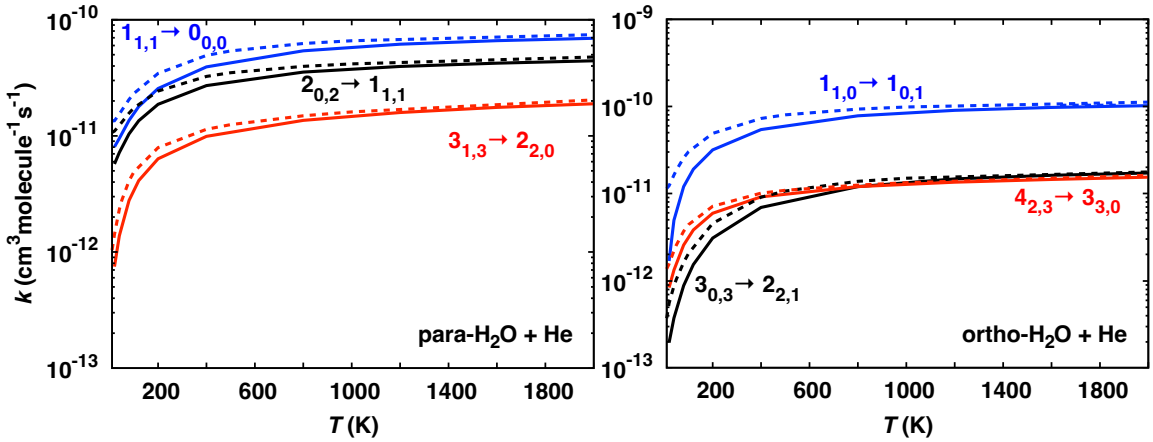

Fig. C.4. Rotational rate coefficient of para-H_2O and ortho-H_2O by He reported by Green et al. (1993) (solid lines), and (Yang et al. 2013) (dashed lines). Rotational transitions of H_2O are labelled as $j^i_{K_a,K_c} \rightarrow j^f_{K_a,K_c}$.